筑波大学
博士 (医学) 学位論文

Protective role of residual *Tet2/Tet3* alleles in development of myeloid leukemia

(残存 *Tet2/Tet3* アレルが骨髄性白血病発症阻止に果たす役割)

2020

筑波大学大学院博士課程人間総合科学研究科

RAKSHA SHRESTHA

Table of contents

Page

1. Abstract

Loss-of-function mutations in ten-eleven translocation-2 *(TET2)* are recurrent events in acute myeloid leukemia (AML) as well as in preleukemic hematopoietic stem cells (HSCs) of age-related clonal hematopoiesis. *TET3* mutations are infrequent in AML, but the level of *TET3* expression in HSCs has been found to decline with age. I examined the impact of gradual decrease of TET function in AML development by generating mice with Tet deficiency at various degrees. $Tet2^{f/f}$ and $Tet3^{f/f}$ mice were crossed with mice expressing *Mx1-Cre* to generate $Tet2^{f/wt}Tet3^{f/f}$*Mx-Cre*$^{+}$ (*T2ΔT3*), $Tet2^{f/f}Tet3^{f/wt}$*Mx-Cre*$^{+}$ (*ΔT2T3*), and $Tet2^{f/f}Tet3^{f/f}$*Mx-Cre*$^{+}$ (*ΔT2ΔT3*) mice. All *ΔT2ΔT3* mice died of aggressive AML at a median survival of 10.7 weeks. By comparison, *T2ΔT3* and *ΔT2T3* mice developed AML at longer latencies, with a median survival of ~27 weeks. Remarkably, all 9 *T2ΔT3* and 8 *ΔT2T3* mice with AML showed inactivation of the remaining nontargeted *Tet2* or *Tet3* allele, respectively, owing to exonic loss in either gene or stop-gain mutations in *Tet3*. Recurrent mutations other than *Tet3* were not noted in any mice by whole-exome sequencing. Spontaneous inactivation of residual *Tet2* or *Tet3* alleles is a recurrent genetic event during the development of AML with Tet insufficiency.

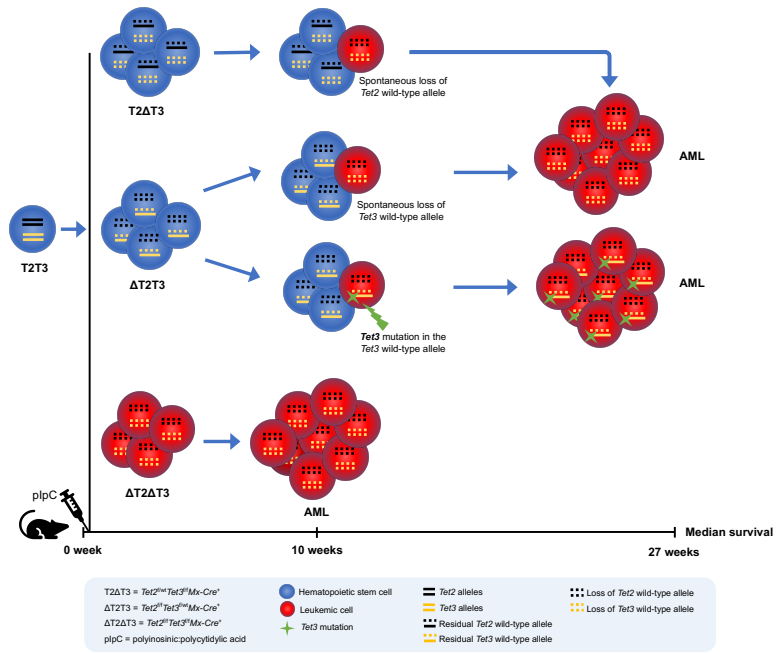

2. Background

2.1 Acute myeloid leukemia

Acute myeloid leukemia(AML) is a heterogeneous form of hematopoietic disorder characterized by infiltration of the bone marrow, blood and other tissues by proliferative and abnormally differentiated cell of the hematopoietic system.[1] AML may arise as a de novo malignancy, due to prior therapy with cytotoxic agents or it may occur in patients with underlying hematological disorders. [2] Approximately 80% cases of AML are seen in adults and it is the most common leukemia in adults in United States[3] and Japan.[4]

Clinical features of AML are mostly due to accumulation of malignant, poorly differentiated myeloid cells within the bone marrow, peripheral blood and other organs. Physical signs and symptoms such as pallor, fatigue, easy bruising, anorexia, weight loss are more common than lymphadenopathy and organomegaly. These are accompanied by anemia, leukocytosis and thrombocytopenia. Morphologically, AML blast cells appear larger than lymphocytes or monocytes and the nuclei are large in size, varied in shape and usually contain several nucleoli. Common cluster differentiation (CD) markers expressed on blasts cell are CD13, CD33 and CD34.[5] The diagnosis of AML is established by the presence of 20% or more blasts in the bone marrow or peripheral blood.[6]

Chromosomal translocations in AML consists of t(8:21) forming the *RUNX1-RUNX1T1* fusion , inv(16) forming *CBFB-MYH11*, and the t(15;17) forming the PML-RARA chimeric protein. [7] Although these cytogenetic abnormalities are important determinants of diagnosis and prognosis in AML, 50-60% of patients have cytogenetically normal AML(CN-AML). [8] In such cases of limited karyotypic abnormality, identification of recurrent gene mutations can be important for further management of AML. Recurrent mutations in AML can be divided according to functional groups as following: genes of the signaling and kinase pathway (FLT3, KIT, KRAS, NRAS, PTPN11, NF1), epigenetic modifiers (DNMT3A, IDH1, IDH2, TET2,

ASXL1 EZH2, MLL/KMT2A), nucleophosmin (NPM1), transcription factors (CEBPA, RUNX1, GATA2), tumor suppressors (TP53), spliceosome complex (SRSF2, U2AF1, SF3B1, ZRSR2) and cohesion complex (RAD21, STAG1, STAG2, SMC1A, SMC3).[9]

The general therapeutic strategy in patients with AML is divided into two phases: induction (cytarabine and anthracycline) and consolidation therapy. The post remission or consolidation strategy is individualized and includes conventional chemotherapy and hematopoietic stem cell transplantation. Though there have been significant improvements in outcomes for younger patients in the past decades, prognosis for those >60 years old remains poor. [10,11]

2.2 *TET* family of genes

Structure

TET1 was initially discovered as a chromosomal translocation partner of the *KMT2A* (previously known as mixed-lineage leukemia (*MLL*)) in leukemia.[12,13] *TET2* and *TET3* were subsequently identified on homology searches. All TET proteins share common features among them (Figure 1); they all consist of a double stranded B helix (DSBH) domain, a cysteine-rich domain, and binding sites for α-ketoglutarate (α-KG) and Fe (II). These structures form the catalytic region in the C terminus. On the amino(N) terminus, *TET1* and *TET3* have a CXXC-type domain that binds to DNA.[14-16]. As for TET2, its ancestral CXXC domain is now encoded separately by a neighboring gene, *IDAX* (also called CXXC4).

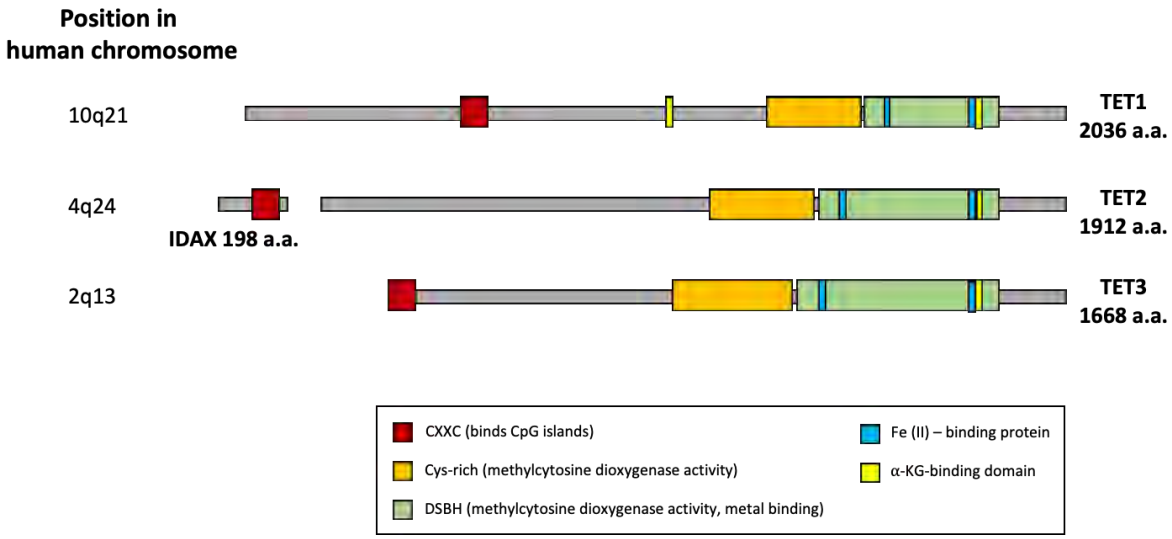

Figure 1: Structure of TET proteins
Structure and functional domains of ten-eleven translocation (TET) family proteins. α-KG, α-ketoglutarate; CD, cysteine-rich domain; Cys, cysteine; DSBH, double-stranded β-helix domain.

TET proteins and DNA methylation

DNA methylation, particularly methylation of cytosine residue at *5'* – Cytosine – phosphate – Guanine – *3'* (CpG) sites, is one of the important epigenetic modification and its disruption can cause dysregulation of gene expression.[17-19] The critical role of TET family proteins in DNA methylation was reported a decade ago. The family of ten-eleven translocation (*TET*) methylcytosine dioxygenases, *TET1, TET2,* and *TET3*, hydroxylate 5-methylcytosine (5-mC) to 5-hydroxymethylcytosine (5-hmC), which is then converted to formylcytosine and carboxylcytosine (Figure 2).[20-23]

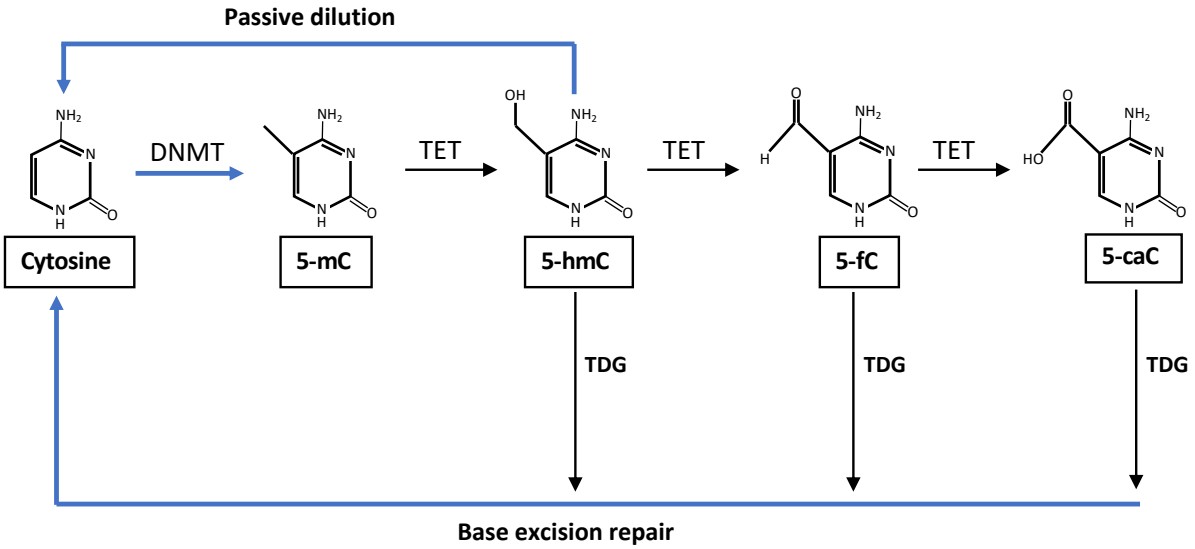

Figure 2: Pathways of cytosine demethylation mediated by ten-eleven translocation (TET) proteins. DNMTs transfer a methyl group to the 5-position of cytosine. TET enzymes catalyze the oxidation of 5-mC to 5-hmC, 5-fC, or 5-caC. All four modified cytosine bases can be demethylated by TDG, then ultimately replaced with unmodified cytosine via base excision repair.
(DNMT, DNA methyltransferase; 5-mC, 5-methylcytosine; 5-hmC, 5-hydroxymethylcytosine; 5-fC, 5-formylcytosine; 5-caC, 5-carboxylcytosine; TDG, thymine DNA glycosylase.)

Physiological functions and expression in solid tumors

TET proteins have roles in diverse biological processes, including epigenetic regulation of gene transcription, embryonic development, stem cell function and cancer, but the mechanisms underlying these roles are still poorly defined. *TET1* and *TET2* play important role in germ cell development via methylcytosine oxidation while *TET3* mediates methylcytosine oxidation in the male pronucleus in the zygote. [24] *TET2* and *TET3* have also shown strong expression in hematopoietic and neuronal lineages. [25]

Mutations of *TET* genes and decreased expression of TET proteins have been implicated in melanoma, colorectal cancer and other cancer including gastric, prostrate, lung, liver and breast cancer. [26 27 28 29]

2.3 *TET* genes in hematological malignancies

The role of TET proteins has been widely studied in hematological malignancies. *TET1* was originally identified as a fusion partner of MLL gene and has been shown to play an oncogenic role in MLL-rearranged AML.[12,13,30] *TET2* loss-of-function mutations have been frequently found in myeloid malignancies such as acute myeloid leukemia (AML; 7.3%–23%)[31-35], chronic myelomonocytic leukemia (CMML; 22%–42%)[31], myelodysplastic syndromes (MDS; 18%–33%)[31,36-38], and myeloproliferative neoplasms (MPN; 7%–16%)[31,39]. Moreover, *TET2* is the second-most frequently mutated gene in age-related clonal hematopoiesis (ARCH).[40-42] These studies suggest that while *TET2* mutations act as strong drivers for myeloid neoplasms, they do not induce any disease by themselves and therefore, concurrence of additional genetic events is necessary for the development of full-blown myeloid malignancies. *TET3* mutations, on the other hand, were found infrequently in myeloid malignancies. mRNA expression of *Tet3*, however, was shown to decline with age in mouse hematopoietic stem cells (HSC) [43], as well as in human peripheral blood T cells.[44]

Taken together, they suggest that the age-dependent decline of TET enzymatic activity through *TET2* mutations and decreased *TET3* expression in HSCs may contribute to the development of myeloid neoplasms, most of which occur in the ageing population. This agrees with the observation that induced deficiency of *Tet2* and *Tet3* led to aggressive development of AML in mice,[45] whereas inactivation of either *Tet2* or *Tet3* alone did not.[46,47] Deficiency of *Tet2* alone in mice led to chronic myelomonocytic leukemia-like diseases[46,48,49], T-cell[50] and B-cell malignancies[51,52] depending upon type of strains. *Tet3* deficiency alone did not significantly disturb hematopoiesis.[47]

3. Aim of the study

In order to understand the mechanisms of leukemic transformation from ARCH through impairment of TET function, I and my colleagues established mice with various degrees of three- and four-allele disruption of *Tet2* and *Tet3.* [53,54] Double homozygous disruption of *Tet2* and *Tet3* led to rapid development of AML, as described previously. [45,53] Mice deficient in three alleles of *Tet2* and *Tet3*, in contrast, progressed to AML after longer latencies.[54] The aim of this study was to explore the molecular mechanism of development of myeloid leukemia in mice with TET deficient status.

4. Materials and methods

4.1 Housing and breeding of mice

Tet2-floxed (*Tet2*$^{f/f}$) mice were provided by Olivier Bernard from INSERM.[46] *Tet3*-floxed (*Tet3*$^{f/f}$) mice were created by Haruhiko Koseki from RIKEN by inserting loxP sites into introns 7 and 9 to delete the cysteine-rich Fe-binding domain (Figure 3A). C57BL/6 (CD45.1) recipients were purchased from CLEA Japan. *Tet2*$^{f/f}$ and *Tet3*$^{f/f}$ mice were crossed with mice expressing *Cre* recombinase under control of the type I interferon-inducible *Mx1* murine promoter (*Mx-Cre*)[55] to obtain *Tet2*$^{f/wt}$*Tet3*$^{f/f}$*Mx-Cre*$^{+}$ (*T2ΔT3*), *Tet2*$^{f/f}$*Tet3*$^{f/wt}$*Mx-Cre*$^{+}$ (*ΔT2T3*), and *Tet2*$^{f/f}$*Tet3*$^{f/f}$*Mx-Cre*$^{+}$ (*ΔT2ΔT3*) mice. Neonatal mice received 3 intraperitoneal injections of polyinosinic:polycytidylic acid (pIpC) at a dose of 300 μg every other day from 2 days after birth. *Tet2*, *Tet3,* and *Mx1-Cre* alleles were genotyped using tail DNA, and the 3 genotypes were distinguished by multiplex PCR (Figure 3B), following previous works in the laboratory (Table 1). [53,54] The mice were housed at the Animal Center for Biomedical Research, University of Tsukuba, following institutional guidelines.

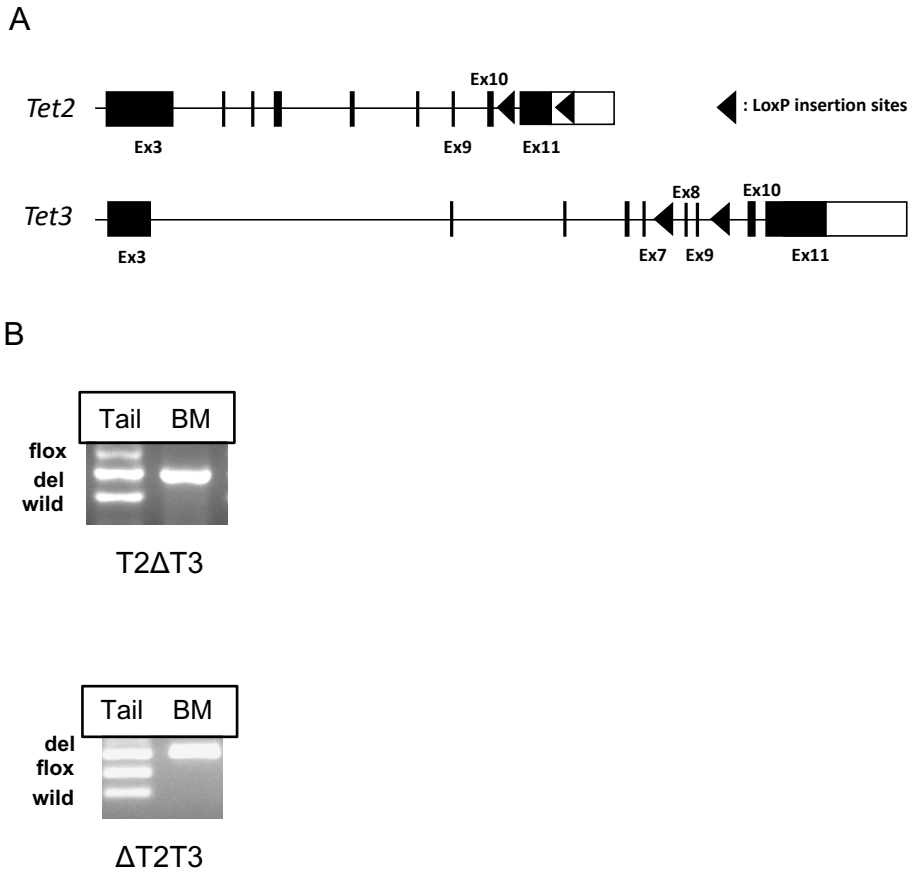

Figure 3: Establishment of *Tet2/Tet3* conditional knockout mice.
(A) Partial structure of *Tet2* and *Tet3* genes. LoxP sites were located in intron 10 and the 3'UTR of exon 11 for *Tet2*, and in introns 7 and 9 for *Tet3*.
(B) Multiplex PCR analyses of *Mx-Cre*-mediated deletion of *Tet2* and *Tet3* alleles in tail and bone marrow (BM) cells. Samples were collected from *Mx-Cre*$^{+}$*Tet2*$^{f/w}$*Tet3*$^{f/f}$ (*T2ΔT3*) or *Mx-Cre*$^{+}$*Tet2*$^{f/f}$*Tet3*$^{f/w}$(*ΔT2T3*) mice 2 months after injections of polyinosinic:polycytidylic acid (pIpC) for tail samples and after development of AML for BM samples.

Tet2 flox F	GGCAGAGGCATGTTGAATGA
Tet2 flox R	TAGACAAGCCCTGCAAGCAAA
Tet2 del R	GTGTCCCACGGTTACACACG
Tet3 flox F	CTAGCACCTCAGTCTGGGACC
Tet3 flox R	TGAGTAAGAGCAGGCAGGGAG
Tet3 del R	CAGACAGTGGCATAGCAGTGG

Table 1: PCR primers used for genotyping and confirmation of *Tet2* and *Tet3* deletion.

4.2 Establishment of cell lines

Bone marrow (BM) cells from leukemic *T2ΔT3* and *ΔT2T3* mice were cultured in Roswell Park Memorial Institute medium (RPMI)-1640 (Sigma) supplemented with 10% fetal bovine serum (FBS), 1% penicillin/streptomycin (PS), and 10 ng/mL murine interleukin-3 (IL-3; Wako) at 37°C and 5% CO_2 for at least 1 month, resulting in the establishment of respective cell lines.

4.3 Quantitative real-time PCR

RNA was isolated using the RNeasy Mini Kit (Qiagen) and transcribed with random hexamers using SuperScript III Reverse Transcriptase (Invitrogen) following the manufacturers' protocols. Quantitative real-time PCR (Q-PCR) was performed using FastStart SYBR Green Master mix or FastStart TaqMan Probe Master mix (Roche) on a 7500 Fast Real-Time PCR system (Applied Biosystems). Relative expression was determined using the relative standard curve method. Each sample was analyzed in triplicate and normalized to 18S RNA. The primers and probes used for this experiment are shown in Table 2. [53]

Tet2 F	CTCGAAAGCGTTCCTCTCTG
Tet2 R	CGGTTGTGCTGTCATTTGTT
Tet3	TaqMan Mm00805754_m1 (Thermo Fisher)
18S	TaqMan Ribosomal RNA Control Reagents (Thermo Fisher)

Table 2. Primers and probes for quantitative real-time PCR (Q-PCR).

4.4 Bone marrow transplantation in mice

BM cells were isolated and flushed with phosphate-buffered saline (PBS) supplemented with 1% bovine serum albumin (BSA) by use of a syringe. For whole BM transplantation, 1 x 10^6 total cells from *T2ΔT3* and *ΔT2T3* mice with 2 x 10^5 BM cells from wild-type CD45.1 mice

were transplanted via the tail vein or orbital sinus into lethally irradiated (4.5 Gy x 2) CD45.1 recipients. At least 2 independent experiments were performed.

4.5 Cell viability assay

The cell lines established from *T2ΔT3* and *ΔT2T3* leukemic mice were treated with decitabine (DAC) at various concentrations for 48 hours. The cell viability was measured by means of a 2-(2-methoxy-4-nitrophenyl)-3-(4-nitrophenyl)-5-(2,4-disulfophenyl)-2H-tetrazolium (WST-8) assay using Cell Counting Kit-8 (Dojindo) following the manufacturer's protocol on a microplate reader (Varioskan Lux, ThermoFisher Scientific).

4.6 Whole exome sequencing

Genomic DNA was extracted from leukemic BM and the corresponding tail from each *T2ΔT3, ΔT2T3,* and *ΔT2ΔT3* leukemic mouse by use of a DNeasy Blood & Tissue kit (Qiagen). Whole exome sequencing (WES) was performed as previously described with help from Seishi Ogawa at Kyoto University.[56] DNA integrity number (DIN) of the genomic DNA of each sample was checked using the Agilent Tapestation 2200. Libraries were prepared with SureSelect XT Mouse All Exon V2 using SureSelect Low Input Reagent Kit (Agilent Technologies) and 200 ng of genomic DNA. The sequencing reads were mapped on GRCm38/mm10 by use of a Burrows-Wheeler Aligner (BWA).[57] Candidate variants were called by the Genomon2 Pipeline (https://github.com/Genomon-Project/GenomonPipeline). Somatic mutations with (i) a Fisher test value >4 and (ii) an Empirical Baysian (EB) call>4 were adopted and filtered by excluding (i) synonymous single nucleotide variants (SNVs), (ii) variants only present in unidirectional reads, (iii) variants located in intergenic, intronic, untranslated regions, and noncoding RNA regions, and (iv) variants occurring in repetitive genomic regions. Candidate mutations were examined by manual inspection with an Integrative Genomics Viewer (IGV) and confirmed by

Sanger sequencing using the primer sets listed in Table 3. In addition, I also applied Copywrite R (version 2.16.0) to data from WES for detection of copy number variation.[58]

Ccdc191 Fwd	GCTCTCGCAAAGGAGCAAAC
Ccd191c Rvs	AGGGAACAGTGTACCTCTCCA
Klk8 Fwd	AACTCTGCCTCTGTTCAGGGT
Klk8 Rvs	GTCCCTGTTGTCCATGGTCTT
Ctnna2 Fwd	GCGGTCTCACATACCCTGAT
Ctnna2 Rvs	GCTGAACAAGTTGAGGTGGC
Tet3 (1) Fwd	ACAAGGGTCATTGGCTCCAG
Tet3 (1) Rvs	CAGGTGGAACAGGAGCAGAG
Tet3 (2) Fwd	GCTGGTAGGGTTGCCATACTT
Tet3 (2) Rvs	TCTCTGCAGGTGATCCGAAG
Msn Fwd	CCCCGGCTTCGGATTAACAA
Msn Rvs	CTGGTGCTTCTCTTCCCGAG
Pdzrn4 Fwd	GCATTGCATGATGGGGGATTC
Pdzrn4 Rvs	TGCAGCTCTCTGCCGTATTG

Table 3. Primers for validation of somatic mutations by sanger sequencing.

4.7 Flow cytometric analysis

BM cells were harvested from femurs and tibiae of mice. Red blood cells were eliminated with ammonium-chloride-potassium (ACK) buffer for 10 minutes at 4 degrees. Cells were washed with 2% fetal bovine serum (FBS) in phosphate-buffered saline (PBS) twice. Cells were incubated with lineage marker antibodies, including biotinylated anti-CD4 (RM4-5, eBioscience), anti-CD8 (53-6.7, eBioscience), anti-B220 (RA3-6B2, eBioscience), anti-Ter119 (TER-119, eBioscience), anti-CD127 (A7R34, Invitrogen) and anti-Gr-1 (RB6-8C5, eBioscience), and then further incubated with phycoerythrin-Cy7 (PE-Cy7)-conjugated anti-Sca-1 antibody (D7, eBioscience), phycoerythrin (PE)-conjugated anti-FcRγ antibody (2.4G2, eBioscience), fluorescein isothiocyanate (FITC)-conjugated anti-CD34 antibody (RAM34,

eBioscience), peridinin-chlorophyll-protein complex (PerCP)-conjugated anti-B220 (RA3-6B2, eBioscience), and peridinin-chlorophyll-protein complex (PerCP)-conjugated streptavidin. Multicolor flow cytometric analysis was performed on BD FACS Aria II (BD Biosciences), and the obtained data were analyzed using FlowJo software (BD Biosciences).

4.8 Histopathologic examination

Peripheral blood cells were collected from the facial veins of leukemic mice. Peripheral blood smears were prepared using cytospin (CF-12D AutoSmear, Sakura). Cells were stained with Wright-Giemsa (Muto Pure Chemicals) for 2 min and then washed with distilled water and dried in air. Cut sections of spleen were fixed with 10% formalin in 0.01 mol/L phosphate buffer (pH 7.2) and embedded in paraffin. Sections were stained with hematoxylin and eosin for histopathologic examination. Cell morphology was examined under a light microscope and photographed using a Keyence BZ X710 microscope (Keyence Corporation).

4.9 Collection of peripheral blood, bone marrow, and spleen

For all experiments mentioned, mice were sacrificed when they appeared sick (indicated by slow movements and weak reactions to external stimuli). Mice with white blood cell count >200 X 10^4/ul and hemoglobin <10 g/dl were considered to be leukemic. Blood was collected from the facial vein into an EDTA-coated Eppendorf tube, smeared onto a slide and air-dried using the cytospin protocol. Automated peripheral blood counts were analyzed using a Celltac α (MEK-6458, Nihon Kohden) according to the manufacturer's instruction. Tibiae, femurs, and pelvises were obtained from mice after cervical dislocation. BM cells were collected by flushing with phosphate-buffered saline (PBS) supplemented with 1% bovine serum albumin (BSA) by use of a syringe. Whole spleens were collected from the mice after they were sacrificed. Splenocytes were prepared by mincing the spleen on a 70-μm cell strainer (BD

Biosciences). Spleen cells were depleted of red blood cells by ACK buffer before flow cytometry.

4.10 PCR for detection of wild-type *Tet2* and *Tet3* alleles

Genomic DNA was isolated using a QIAmp DNA Mini Kit (Qiagen) from the BM and tails of leukemic mice. Twenty nanograms of DNA template was mixed with a 20-ul reaction mixture containing 2 ul of 10X PCR buffer, 1.6 ul of dNTP, 1 ul of each primer, 0.1 ul of Taq polymerase, and 12.3 ul of distilled water for detection of wild-type *Tet2* allele. Polymerase chain reaction for *Tet2* was performed using Taq polymerase (Takara) under the following conditions: (95^{o}C: 1 min, [95^{o}C: 30s; 58^{o}C: 30s; 72^{o}C: 30s] x 35 cycles, 72^{o}C: 30s). Similarly, 20 ng of DNA template was mixed with a 24-ul reaction mixture containing 2.5 ul of 10X PCR buffer, 2.5 ul of dNTP, 1.5 ul of $MgSO_4$, 0.4 ul of each primer, 0.5 ul of KOD-plus-neo polymerase, and 15.8 ul of distilled water for detection of wild-type *Tet3* alleles. Polymerase chain reaction for *Tet3* was performed using KOD-plus-neo polymerase (Toyobo) under the following conditions: (94^{o}C: 2min, [98^{o}C: 10s, 74^{o}C: 30s] x 5 cycles; [98^{o}C: 10s, 72^{o}C: 30s] x 5 cycles; [98^{o}C: 10s, 70^{o}C: 30s] x 5 cycles; [98^{o}C: 10s, 68^{o}C: 30s] x 25 cycles). Primers used are shown in Table 1. The resultant PCR products of BM were placed aside the corresponding tail in 3% agarose gel to observe the status of wild-type alleles of *Tet2* or *Tet3*. Samples subjected to PCR are mentioned in Table 4.

4.11 Validation of somatic mutations

Candidate somatic mutations identified by exome sequencing were validated by Sanger sequencing (Figure 14). Primers for the somatic mutations were identified using the UCSC genome browser. Primers used are shown in Table 3. Twenty nanograms of genomic DNA extracted from the BM and tails of leukemic mice were subjected to PCR using KOD plus neo

(Toyobo) with these primers under the following conditions: ([94°C: 2 min; 98°C: 10s, 74°C: 30s] x 5 cycles; [98°C: 10s, 72°C: 30s] x 5 cycles; [98°C: 10s, 70°C: 30s] x 5 cycles; [98°C: 10s, 68°C: 30s] x 30 cycles; 68°C: 7 mins). Direct Sanger sequencing was performed with the PCR product. Sanger sequencing was performed on a Genetic Analyzer (Applied Biosystems® 3130xl and 3500 Genetic Analyzer), and the variant sequences were analyzed using Genetyx version 13.1.0 (Genetyx) and Chromas version 2.6.6 (Technelysium). Then, the sequence was confirmed using the UCSC Genome Browser Blat tool.[59]

4.12 Statistical analysis

Results are expressed as mean ± standard error of the mean. Significant differences between the results were assessed by using an analysis of variance on Prism (GraphPad Software, version 6). Probability values <.05 were considered significant. A log rank test was used for survival curve analysis. Correlations of messenger RNA (mRNA) expression levels were evaluated by calculating the Pearson correlation coefficient.

5. Results

5.1 Both *T2ΔT3* and *ΔT2T3* mice develop AML with longer latencies than those of *ΔT2ΔT3* mice

Mice with various degrees of deficiency of *Tet2* and *Tet3* were generated to investigate whether and how insufficient levels of TET enzymes affect the development of leukemia: $Tet2^{f/f}Tet3^{wt/wt}Mx\text{-}Cre^{+}$ (*ΔT2*), $Tet2^{wt/wt}Tet3^{f/f}Mx\text{-}Cre^{+}$ *(ΔT3)*, $Tet2^{f/wt}Tet3^{f/wt}Mx\text{-}Cre^{+}$ *(T2T3),* $Tet2^{f/wt}Tet3^{f/f}Mx\text{-}Cre^{+}$ (*T2ΔT3*), $Tet2^{f/f}Tet3^{f/wt}Mx\text{-}Cre^{+}$ (*ΔT2T3*), and $Tet2^{f/f}Tet3^{f/f}Mx\text{-}Cre^{+}$ (*ΔT2ΔT3*) mice. Sufficient excision of floxed alleles following pIpC injection was observed in BM cells (Figure 3B). *ΔT2ΔT3* mice died after a median survival of 10.7 weeks (range, 5.42–15.42 weeks; n = 41; Figure 4), an observation very similar to the one previously reported.[45]

In contrast, both *T2ΔT3* and *ΔT2T3* mice died after a longer median survival (27.2 and 28.0 weeks; range, 8.8–45.7 and 17.8–45.5 weeks; n = 51 and n = 47, respectively; p = 0.0001 for both; Figure 4). Approximately half of the *ΔT2* mice died at 80 weeks from CMML-like disease, as previously described in these mice,[46] whilst much smaller fractions of *ΔT3* (7%) and *T2T3* mice (12%) died at similar observation periods (Figure 4). A part of the aforementioned results was produced by Koichiro Maie (a proportion of data of survival of *ΔT2ΔT3* mice) and Masatomo Ishihara (a proportion of data of survival of *ΔT2, ΔT3, T2ΔT3, ΔT2T3, and T2T3* mice) and were included in their theses. [53 54]

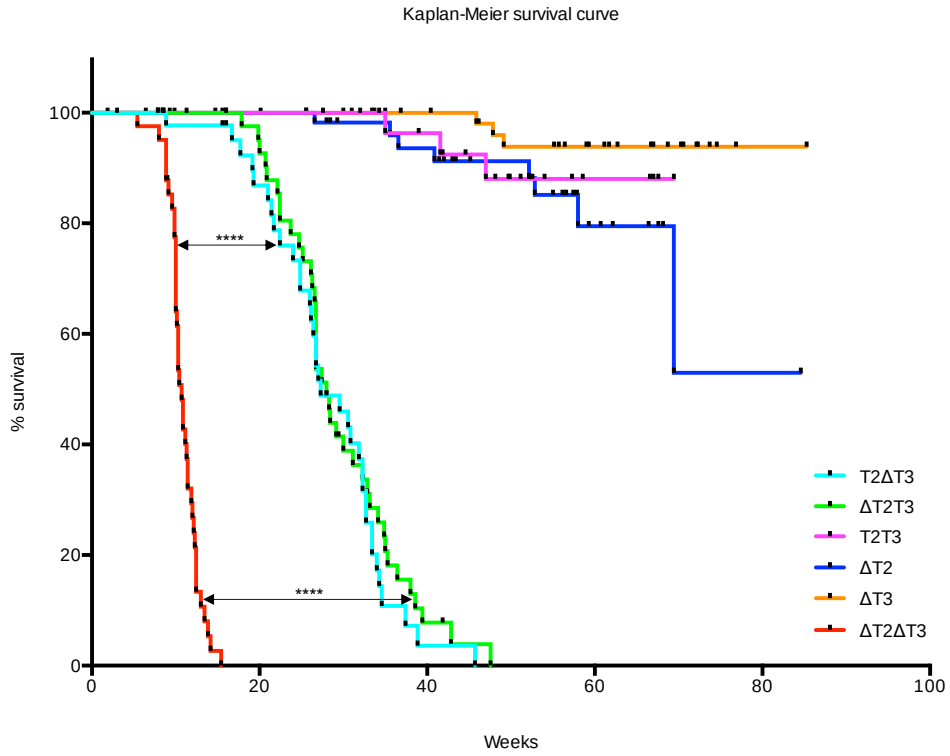

Figure 4: Survival curves of mice with Tet insufficiency.
Kaplan-Meier survival curves of *ΔT2ΔT3* (*Mx1-Cre*$^{+}$*Tet2*$^{f/f}$*Tet3*$^{f/f}$; n = 47); *T2ΔT3* (*Mx1-Cre+Tet2*$^{f/w}$*Tet3*$^{f/f}$; n = 57); *ΔT2T3* (*Mx1-Cre+Tet2*$^{f/f}$*Tet3*$^{f/w}$; n = 52); *T2T3* (*Mx1-Cre*$^{+}$*Tet2*$^{f/w}$*Tet3*$^{f/w}$; n = 38); *ΔT2* (*Mx1-Cre+Tet2*$^{f/f}$*Tet3*$^{wt/wt}$, n = 61); and *ΔT3* (*Mx1-Cre*$^{+}$*Tet2*$^{wt/wt}$*Tet3*$^{f/f}$, n = 78) mice. ****$P < .0001$. A part of the above results was produced by Koichiro Maie (survival of *ΔT2ΔT3* mice) and Masatomo Ishihara (survival of *ΔT2, ΔT3, T2ΔT3, ΔT2T3, and T2T3* mice). [53,54]

Marked peripheral blood leukocytosis, thrombocytopenia, and anemia accompanied by massive splenomegaly were observed in all sacrificed *T2ΔT3*, *ΔT2T3*, and *ΔT2ΔT3* mice. These findings and the blast-like morphology on microscopic observation suggested development of acute leukemia (Figure 5A, 5B). Koichiro Maie produced a part of these results related to *ΔT2ΔT3* mice and Masatomo Ishihara produced a part of these results related to control, *T2ΔT3* and *ΔT2T3* mice.[53,54]

A

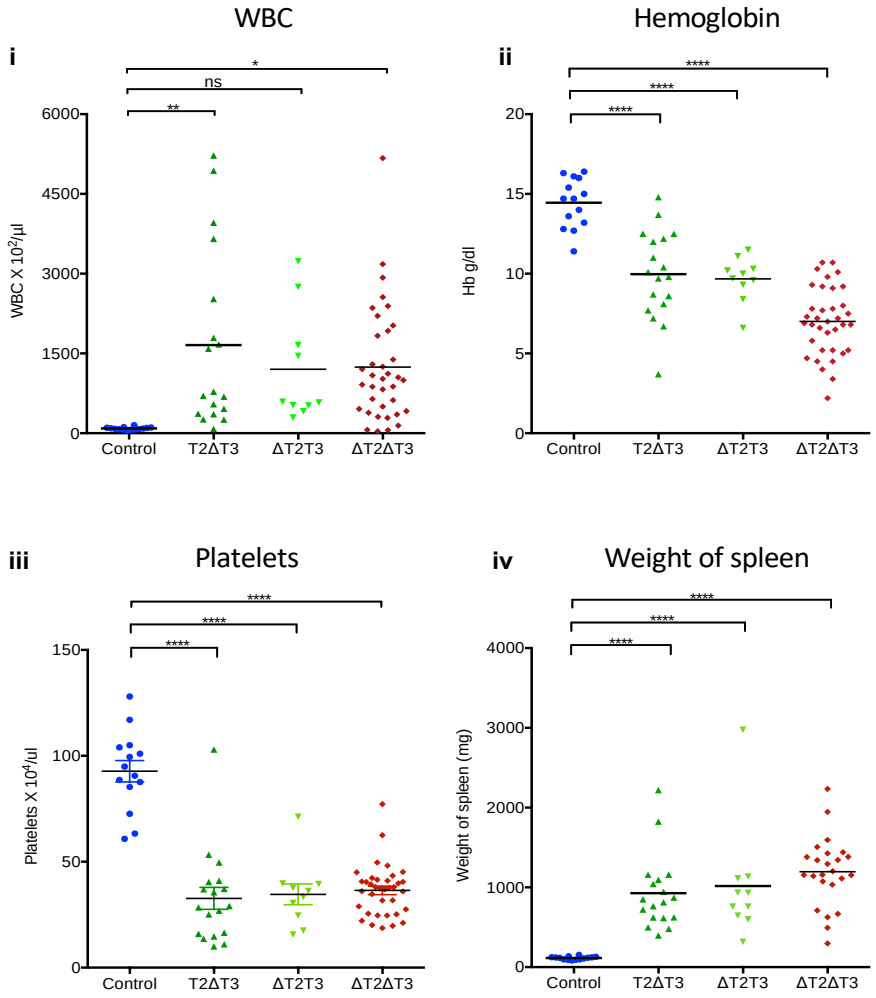

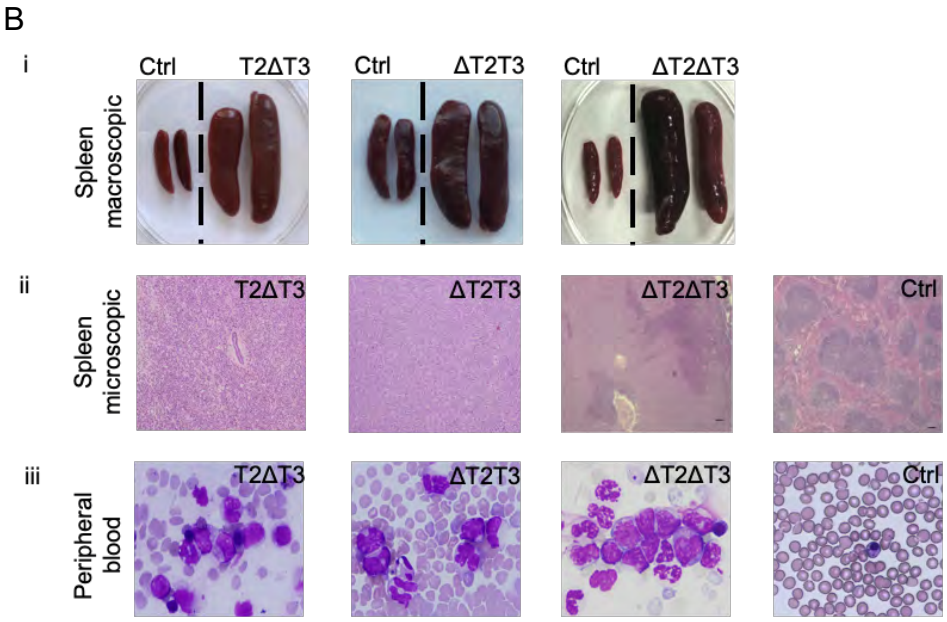

Figure 5: Characteristics of leukemia in *T2ΔT3, ΔT2T3,* and *ΔT2ΔT3* mice.
(A) WBC counts (i), hemoglobin levels (ii), and platelet counts (iii) of *T2ΔT3* (n = 18), *ΔT2T3* (n = 10), and *ΔT2ΔT3* (n = 36) mice and of *Mx1-Cre*$^{-}$*Tet2f/fTet3f/w*, *Tet2f/wTet3f/f*, or *Tet2f/fTet3f/f* mice (Control; n = 14), and spleen weights (iv) of *T2ΔT3* (n = 18), *ΔT2T3* (n = 10), and *ΔT2ΔT3* (n = 24) mice and of control mice (n = 14). (B) (i) Representative macroscopic photographs of spleen from leukemic *T2ΔT3, ΔT2T3,* and *ΔT2ΔT3* mice. (B) (ii) Representative microscopic photographs showing obliteration of the normal spleen architecture in *T2ΔT3, ΔT2T3,* and *ΔT2ΔT3* mice (hematoxylin and eosin stain; original magnification ×10). (B) (iii) Peripheral blood smear showing blast-like morphology from representative *T2ΔT3, ΔT2T3,* and *ΔT2ΔT3* mice (Wright Giemsa stain; original magnification ×40). **P* < .05, ***P* < .01, *****P* < .0001. ns, not significant. Koichiro Maie and Masatomo Ishihara included a part of the above results in their theses. [53,54]

Leukemic BM in all 18 *T2ΔT3*, 10 *ΔT2T3*, and 18 *ΔT2ΔT3* mice showed c-Kit^{+} cells positive for CD16/32 and CD34 (Figure 6A), although there was also an increase in cells of unknown origins expressing CD3 in peripheral blood of 3 of the 18 *T2ΔT3* and 2 of the 10 *ΔT2T3* mice (Figure 6B). Therefore, despite the difference in latency, the majority of the *T2ΔT3* and *ΔT2T3* mice developed AML with a similar phenotype as that in all the *ΔT2ΔT3* mice. A part of these data were included in doctoral dissertation by Koichiro Maie (*ΔT2ΔT3)* and master's thesis by Masatomo Ishihara (*T2ΔT3*, *ΔT2T3)* [53,54], while a significant proportion of the data was produced by me as shown in the Figure 6.

A

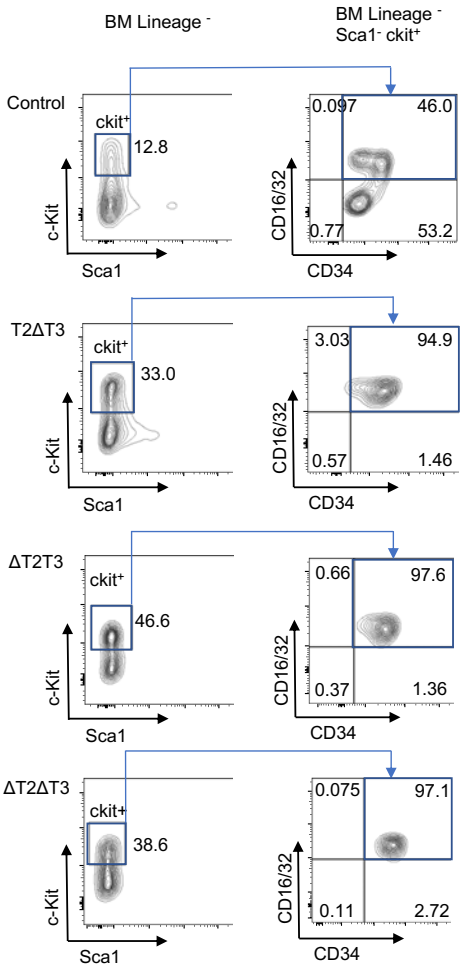

B

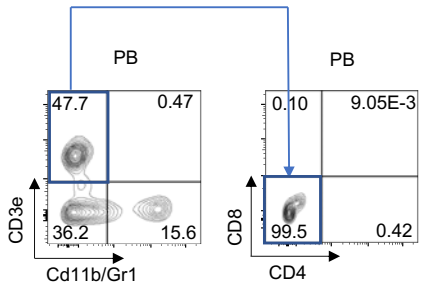

Figure 6: Flow cytometry analysis of primary bone marrow cells.
(A) Flow cytometry analysis of BM from representative leukemic *ΔT2ΔT3, T2ΔT3,* and *ΔT2T3* mice for c-Kit, Sca1, CD16/32, and CD34. (B) CD3 cells seen in peripheral blood of some *T2ΔT3* and *ΔT2T3* mice. (ckit = marker for hematopoietic progenitors in the bone marrow, sca-1 = marker for hematopoitic stem cell, CD16/23 = marker for B cells, monocytes/macrophages, granulocytes, CD34 = marker for hematopoitic stem cells, CD3e = marker for T cells, CD4 = marker for T helper cells, CD8 = marker for cytotoxic T cells.)

I confirmed the penetrance of AML via transplantation of BM cells of leukemic *T2ΔT3* and *ΔT2T3* mice to irradiated congenic mice (Figures 7A, 7B). Results relevant to *ΔT2ΔT3* mice were included in Koichiro Maie's doctoral dissertation. [53]

A

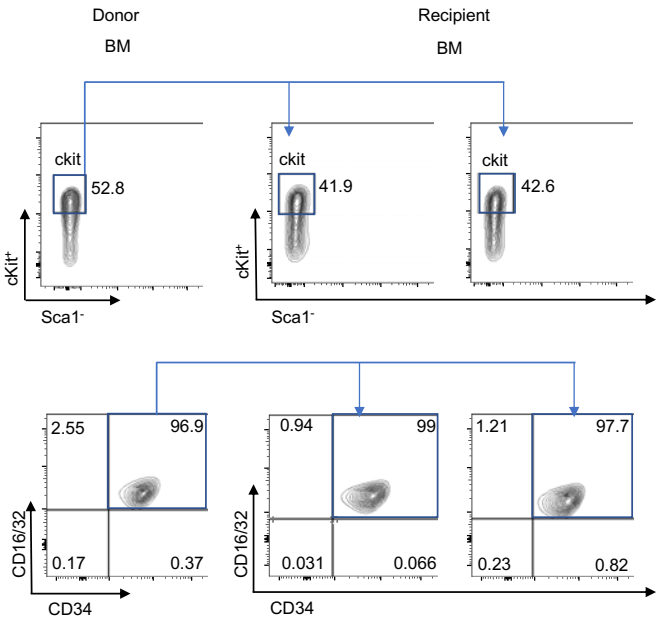

B

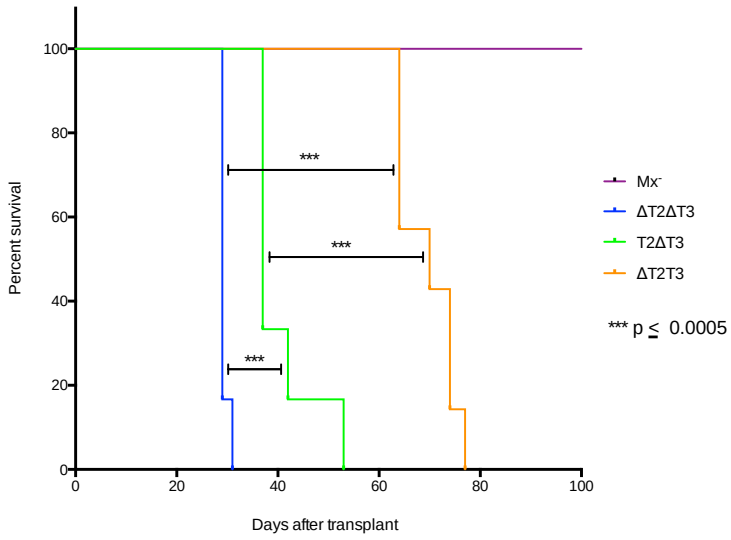

Figure 7: Bone marrow transplantation.
(A) Representative flow cytometric analysis of recipient BM cells after transplantation of *T2ΔT3, ΔT2T3,* and *ΔT2ΔT3* leukemic BM cells. (B) Kaplan-Meier survival curves of Mx$^-$ (n = 5), *ΔT2ΔT3* (*Mx1-Cre*$^+$*Tet2*$^{f/f}$ *Tet3*$^{f/f}$, n = 6); *T2ΔT3* (*Mx1-Cre*$^+$*Tet2*$^{f/w}$ *Tet3*$^{f/f}$, n = 6); *ΔT2T3* (*Mx1-Cre*$^+$*Tet2*$^{f/f}$ *Tet3*$^{f/w}$, n = 7) mice. ***$P \leq 0.0005$. Data relevant to *ΔT2ΔT3* mice were published in Koichiro Maie's doctoral dissertation. [53]

Whole BM cells from *T2ΔT3*, *ΔT2T3*, and *ΔT2ΔT3* mice with AML were easily propagated in liquid culture supplemented with IL-3 for at least 3 months. The cell lines showed c-Kit^{+} cells partially positive for CD16/32 and CD34 that were similar in characteristics to the primary leukemic bone marrow cells (Figure 8). A part of data related to *ΔT2ΔT3* mice were included in Koichiro Maie's doctoral dissertation. [53]

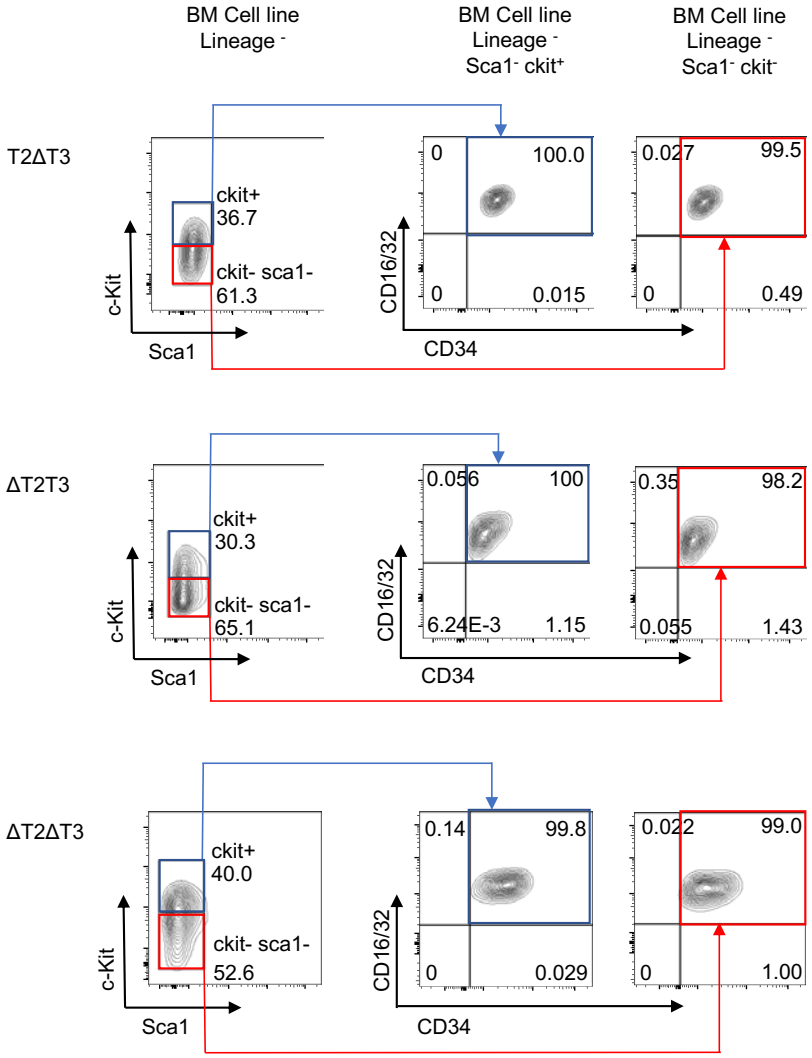

Figure 8: Characterization of cell lines from different genotypes
Representative figure of cell lines established from *T2ΔT3 (Mx1-Cre^{+}Tet2$^{f/w}$ Tet3$^{f/f}$)*; *ΔT2T3* (*Mx1-Cre^{+}Tet2$^{f/f}$ Tet3$^{f/w}$*) and *ΔT2ΔT3* (*Mx1-Cre^{+}Tet2$^{f/f}$ Tet3$^{f/f}$*) mice showing characteristics similar to the primary leukemic bone marrow cells.

When treated with the hypomethylating agent (HMA) decitabine, cell growth was dose-dependently inhibited in all AML cell lines examined (Figure 9). The sensitivity was similar irrespective of the genotype of the mice from which the cell lines were derived (Figure 9). Koichiro Maie produced the data relevant to to *ΔT2ΔT3* mice and included them in his dissertation.[53]

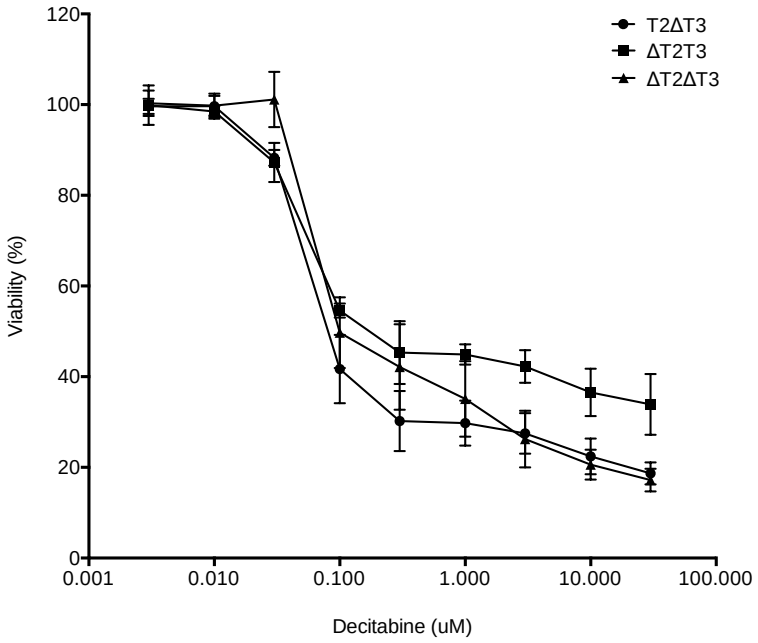

Figure 9: Effects of hypomethylating agents *in vitro.*
Cell viability assay of representative *T2ΔT3, ΔT2T3,* and *ΔT2ΔT3* leukemic cell lines under treatment with decitabine (DAC) for 48 hours. Shown are representative results from 3 independent experiments. Error bars are shown. Data relevant to *ΔT2ΔT3* mice were produced by Koichiro Maie. [53]

In summary, *T2ΔT3* and *ΔT2T3* mice with three-allele disruption in *Tet2* and *Tet3* developed AML, with significantly longer latencies than those with four-allele disruption. AML cells arising from the three-allele disrupted *T2ΔT3* and *ΔT2T3* mice presented an indistinguishable phenotype similar to the phenotype that developed in the four allele-disrupted *ΔT2ΔT3* mice.

5.2 Inactivation of the *Tet2* or *Tet3* non-targeted allele is a recurrent clonal event

Quantitative PCR of leukemic BM cells of *T2ΔT3, ΔT2T3* and *ΔT2ΔT3* mice was performed. Leukemic cells from *T2ΔT3* mice (n = 7) and *ΔT2ΔT3* mice (n=7) demonstrated very low levels of *Tet2* (exon 10–11 region) expression (Figure 10A). The leukemic BM cells from 2 of the 4 *ΔT2T3* mice showed low levels of *Tet3* (exon 7–8 region) expression, similar to those in the leukemic BM cells of the *ΔT2ΔT3* mice. The other two samples among the *ΔT2T3* mice (#47 and #60) showed expression of *Tet3* at a level similar to the control mice (Figure 10B).

A

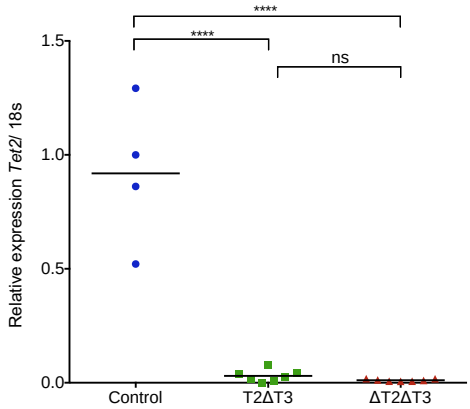

B

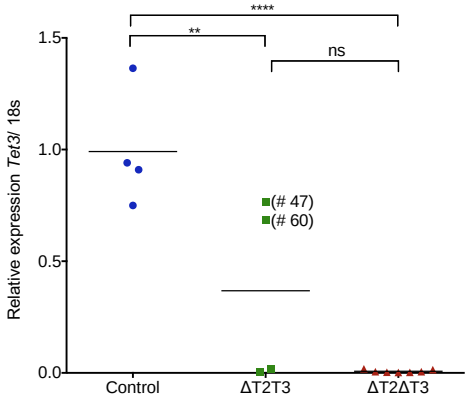

Figure 10: Quantitative real-time PCR (Q-PCR) analysis.
Q-PCR analysis of *Tet2* (A) and *Tet3* (B) transcript levels in leukemic BM cells from *T2ΔT3* (n = 7), *ΔT2T3* (n = 4), and *ΔT2ΔT3* (n = 7) mice and in whole BM cells from *Mx1-Cre*$^{-}$ *Tet2*$^{f/f}$*Tet3*$^{f/w}$, *Tet2*$^{f/w}$*Tet3*$^{f/f}$, or *Tet2*$^{f/f}$*Tet3*$^{f/f}$ mice (Control; n = 4). The results are normalized to 18S rRNA and shown relative to the levels seen in the control samples. The presence of residual *Tet3* (exon 7–8 region) transcript is denoted as #47 and #60. ****$P < 0.0001$.

I prepared DNAs from the leukemic BM cells of the *T2ΔT3* and *ΔT2T3* mice and from their respective tails and applied them to multiplex PCR to analyze the status of the *Tet2* and *Tet3* alleles. All 9 *T2ΔT3* and 6 of the 8 *ΔT2T3* mice showed lack of amplification of the sequences corresponding to the loxP-targeted regions: exon 11 of *Tet2* and exons 8 and 9 of *Tet3*, respectively whereas these exons were amplified in the tail DNAs (Figure 11). Exons 8 and 9 of *Tet3* were amplified in 2 AML samples from *ΔT2T3* mice (#47 and #60) (Figure 11B).

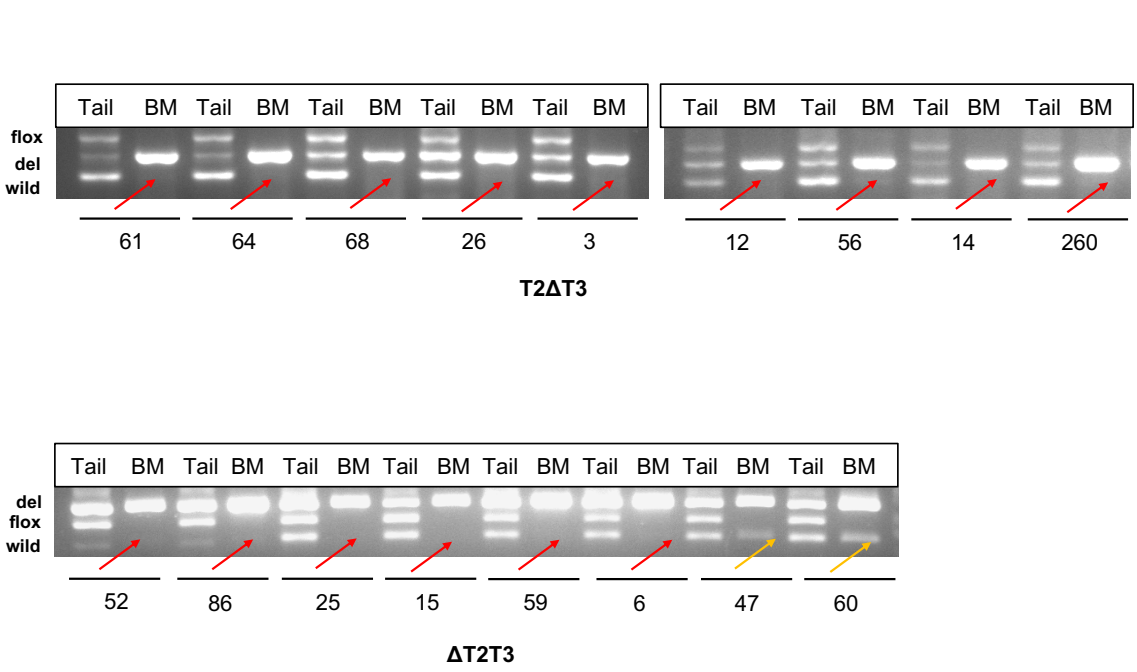

Figure 11: Multiplex polymerase chain reaction (PCR) of leukemic BM with respective tails from *T2ΔT3* and *ΔT2T3* mice.
Multiplex PCR was performed for the regions spanning the *loxP* sites on *Tet2* (exon 11) and *Tet3* (exons 8 and 9) in the BM and tail DNAs of *T2ΔT3* (n = 9) (A) and *ΔT2T3* (n = 8) (B) mice respectively. Lack of amplification of the *Tet2* and *Tet3* wild-type allele in BM from *T2ΔT3* (n = 9) and *ΔT2T3* (n = 6) mice, respectively, is highlighted with red arrows. Amplification of the *Tet3* wild-type allele in BM from *ΔT2T3* mice (n=2; #47 and #60) is highlighted with yellow arrows. flox, del, and wild: PCR products representing floxed, deleted, and wild-type alleles, respectively.

I further performed WES for DNAs from leukemic BM cells with their respective tail DNAs from *T2ΔT3* (n = 6), *ΔT2T3* (n = 8), and *ΔT2ΔT3* (n = 4) mice (Table 4). I then applied BWA alignment and Genomon2 pipeline to the obtained data. The mean sequence depth for all samples was 90X (Figure 12). I identified 10 non-silent somatic mutations in 9 genes in 9 leukemic BM samples from three-allele disrupted mice with AML (n = 14) (Table 5 and 6). Seven of 10 mutations were analyzed and confirmed by Sanger sequencing (Figure 13 and 14). I did not identify any somatic SNVs in the leukemic BM samples from four-allele disrupted mice (n = 4) (Figure 13; Table 5). Surprisingly, recurrent mutations were found only in the *Tet3* gene in leukemic BM samples from *ΔT2T3* mice (n=2; #47 and #60). These were stopgain SNVs at exons 5 (#47) and 6 (#60). Both of these nonsense mutations resulted in loss of the catalytic domain of *Tet3* (Figure 13c; Table 6).

Sample	Genotype	PCR	WES
61	T2ΔT3	+	+
64	T2ΔT3	+	+
68	T2ΔT3	+	+
26	T2ΔT3	+	+
3	T2ΔT3	+	+
12	T2ΔT3	+	+
56	T2ΔT3	+	-
14	T2ΔT3	+	-
260	T2ΔT3	+	-
52	ΔT2T3	+	+
86	ΔT2T3	+	+
25	ΔT2T3	+	+
15	ΔT2T3	+	+
59	ΔT2T3	+	+
6	ΔT2T3	+	+
47	ΔT2T3	+	+
60	ΔT2T3	+	+
25A	ΔT2ΔT3	+	+
26A	ΔT2ΔT3	+	+
54A	ΔT2ΔT3	+	+
29A	ΔT2ΔT3	+	+

Table 4: Samples subjected to PCR and WES.

A

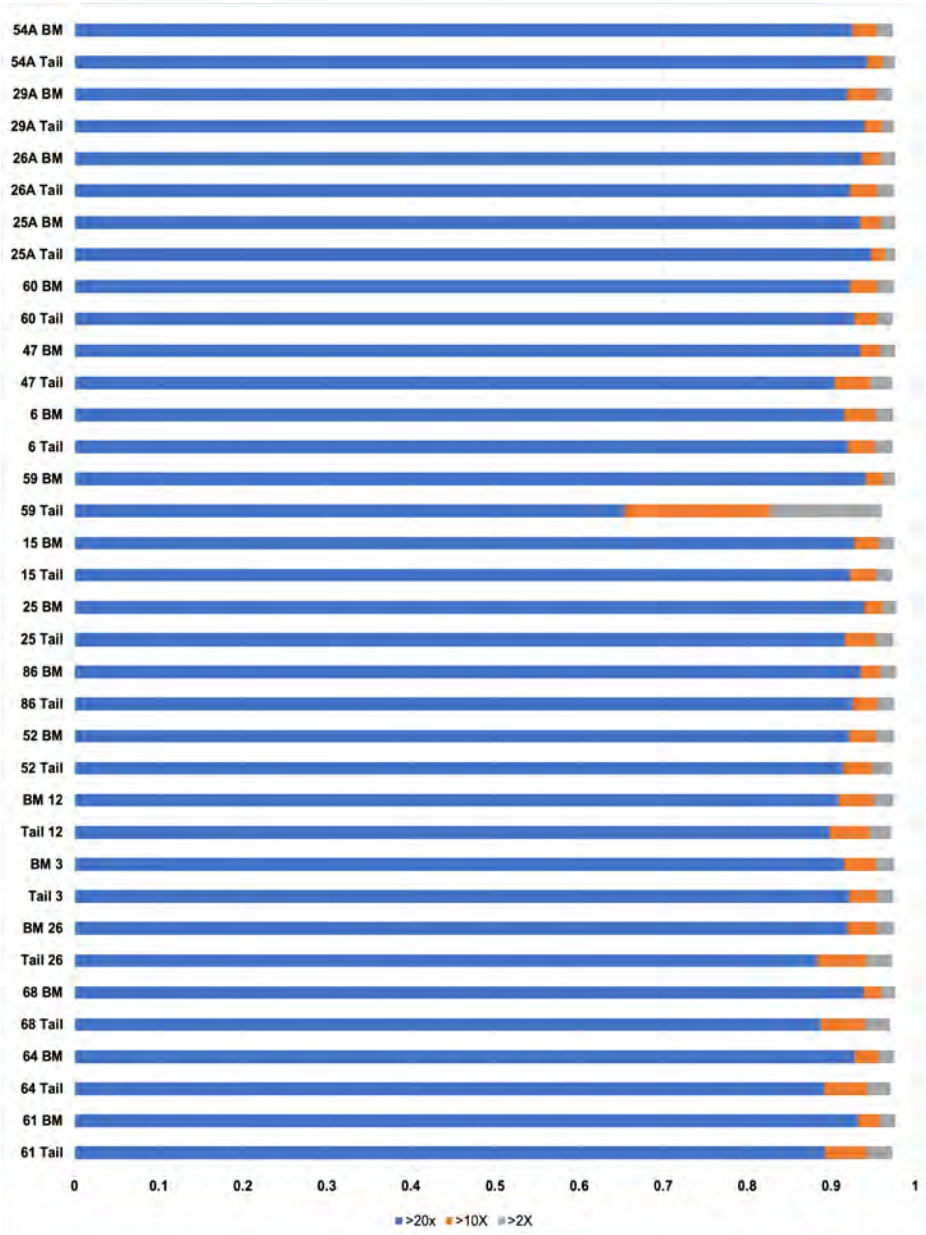

B

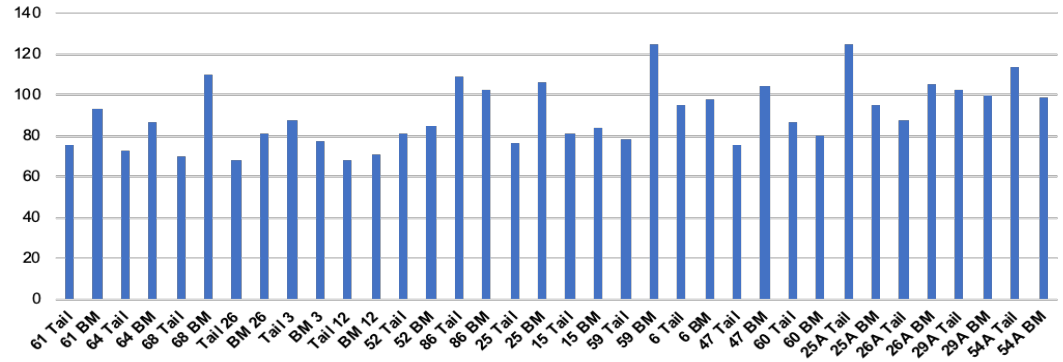

Figure 12: Coverages of whole exome sequencing.
(A) The coverage of the targeted region is plotted for 18 paired samples (tail and BM); Y axis = sample, X axis = ratio of coverage, 1= 100%. (B) The average depths of the 18 paired samples (tail and BM) are shown.

ID	Genotype	Chromosome	Gene	VAF
BM 61	T2ΔT3	-	-	-
BM 64	T2ΔT3	-	-	-
BM 68	T2ΔT3	7	Klk8	0.458
BM 26	T2ΔT3	-	-	-
BM 3	T2ΔT3	5	Tmem132b	0.466
BM 12	T2ΔT3	X	Msn	0.500
BM 47	ΔT2T3	6	Tet3	0.536
BM 52	ΔT2T3	6	Ctnna2	0.226
BM 86	ΔT2T3	16	Ccdc191	0.271
BM 60	ΔT2T3	6	Tet3	0.455
BM 60	ΔT2T3	15	Pdzrn4	0.567
BM 25	ΔT2T3	5	Setd1b	0.466
BM 15	ΔT2T3	-	-	-
BM 59	ΔT2T3	-	-	-
BM 6	ΔT2T3	9	Megf11	0.513
BM 25A	ΔT2ΔT3	-	-	-
BM 26A	ΔT2ΔT3	-	-	-
BM 54A	ΔT2ΔT3	-	-	-
BM 29A	ΔT2ΔT3	-	-	-

Table 5: Mutations identified by WES
Red font indicates *Tet3* genes identified on exome sequencing.
VAF, variant allele frequency.

Table 6: Details of mutations identified on Whole Exome Sequencing (WES).

Genotype	ID	Chrom	Position	Ref	Variant	Gene ID	Exonic Function	Reference Sequence	Amino acid change	Protein change	depth_ tumor	variantNum_ tumor	depth_ normal	variantNum_ normal	misRate_ tumor	P-value (fisher)	P-value (fisher_ realign ment)	P-value (EBCall)
T2ΔT3	BM 68	chr7	43803695	G	A	Klk8	nonsynonymous SNV	NM_008940: exon5	c.G709A	p.E237K	83	38	35	2	0.458	4.93	4.851	6.927
T2ΔT3	BM 3	chr5	125698694	G	A	Tmem132b	nonsynonymous SNV	NM_001190352: exon4	c.G1231A	p.V411I	58	27	69	2	0.466	8.567	8.567	60
T2ΔT3	BM 12	chrX	96160175	C	T	Msn	nonsynonymous SNV	NM_010833: exon8	c.C883T	p.R295C	52	26	41	2	0.5	5.991	5.991	14.199
ΔT2T3	BM 60	chr6	83376857	G	A	Tet3	stopgain	NM_001347313: exon7	c.C2821T	p.R941X	55	25	44	3	0.455	4.84	5.188	14.169
ΔT2T3	BM 60	chr15	92770087	G	T	Pdzrn4	stopgain	NM_001164594: exon8	c.G1402T	p.E468X	30	17	27	2	0.567	4.121	4.121	13.827
ΔT2T3	BM 25	chr5	123161122	C	A	Setd1b	stopgain	NM_001040398: exon12	c.C5220A	p.Y1740X	58	27	30	1	0.466	4.699	5.023	12.141
ΔT2T3	BM 6	chr9	64506123	G	A	Megf11	nonsynonymous SNV	NM_001134399: exon3	c.G191A	p.R64Q	78	40	68	3	0.513	10.041	10.217	60
ΔT2T3	BM 47	chr6	83379895	G	A	Tet3	stopgain	NM_001347313: exon6	c.C2680T	p.R894X	56	30	35	1	0.536	6.763	6.71	6.746
ΔT2T3	BM 52	chr6	76954803	C	A	Ctnna2	stopgain	NM_001355193: exon13	c.G1813T	p.E605X	62	14	68	0	0.226	4.876	4.816	4.02
ΔT2T3	BM 86	chr16	43939110	G	A	Cedc191	nonsynonymous SNV	NM_027801: exon8	c.G1273A	p.G425S	96	26	88	2	0.271	6.034	5.927	4.838

A

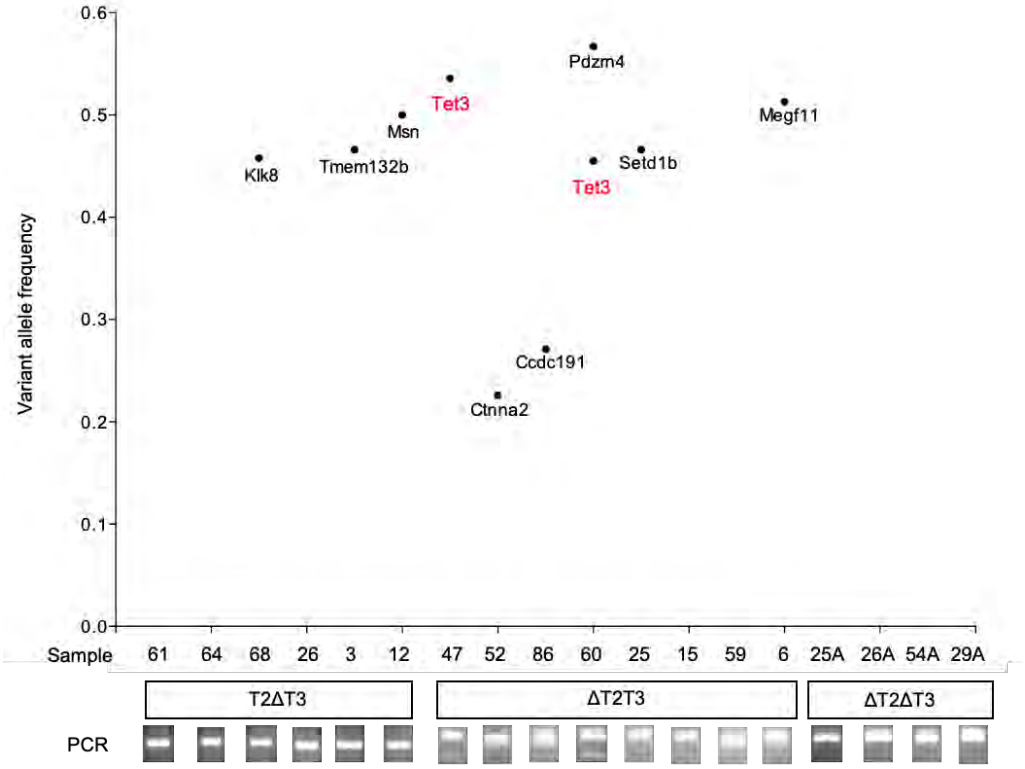

B

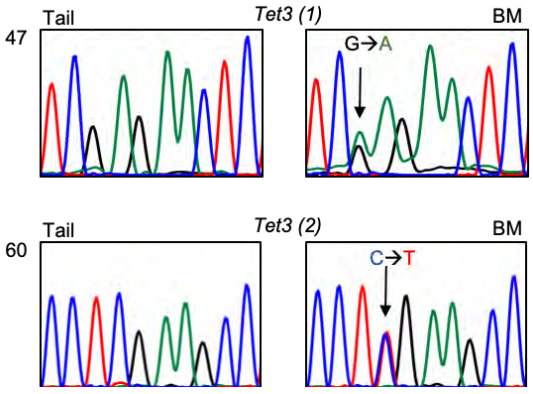

C

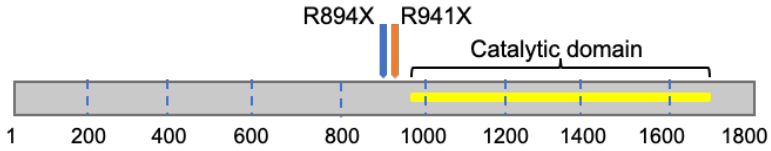

Figure 13: Whole exome sequencing (WES) of *T2ΔT3*, *ΔT2T3*, and *ΔT2ΔT3* mice.
(A) Variant allele frequency plot of mutations revealed by WES of paired tail and BM samples from *T2ΔT3*, *ΔT2T3*, and *ΔT2ΔT3* mice. Amplification of the *Tet3* wild-type allele in BM from *ΔT2T3* mice (n = 2; #47 and #60) is highlighted with yellow arrows as shown in Figure 11. (B) Validation of *Tet3* mutations identified in WES by Sanger sequencing. (C) Position of *Tet3* mutations revealed by exome sequencing in samples #47 (R894X) and #60 (R941X) are shown in the *Tet3* gene.

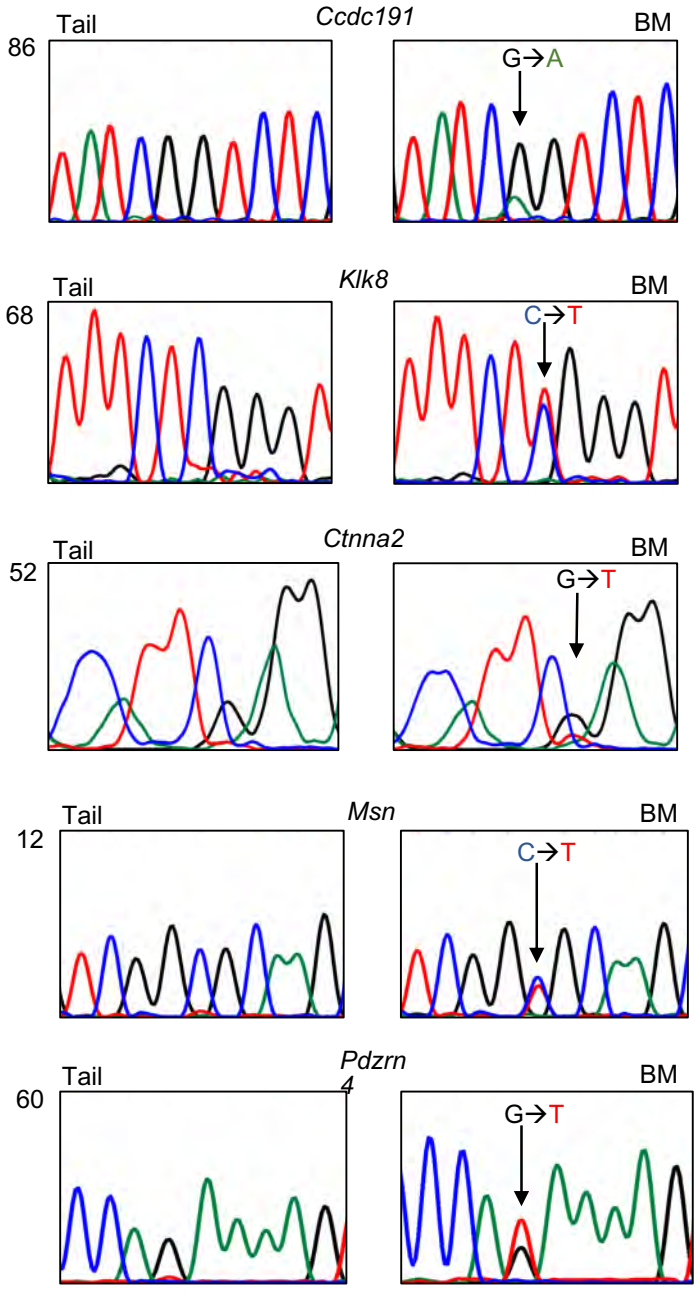

Figure 14: Validation of mutations identified on whole exome sequencing by Sanger sequencing. Candidate mutations found by whole exome sequencing (WES) were examined by Sanger sequencing for DNAs of leukemic BM and tails as a reference. Change in the base is shown with alphabetical letters in the color corresponding to the base sequence.

When I manually inspected the data from WES on IGV, I observed an absence of reads on exon 11 of *Tet2* in all the *T2ΔT3* mice-derived AML samples (n = 6; Figure 15A), which corresponded to the absence of amplification in PCR (Figure 11A). Similarly, the sequencing reads of exons 8 and 9 of *Tet3* were absent in 6 of the 8 AML samples from *ΔT2T3* mice (n = 6) (Figure 15B), which also corresponded to their absence of amplification in PCR (Figure 17B). IGV inspection revealed reads of exons 8 and 9 of *Tet3* in 2 samples from *ΔT2T3* mice, in which somatic *Tet3* nonsense SNVs were identified (#47 and #60, Figure 15B). Copy number analysis of the WES data did not detect deletion involving either *Tet2* or *Tet3* (Figure 16). It was concluded that inactivation of residual non-targeted alleles of *Tet2* or *Tet3* is an extremely recurrent event that leads to AML development. Inactivation was due to loss of exon(s) corresponding to the loxP-targeted regions in the non-targeted allele (in most of the three allele-disrupted mice-derived AML) or due to loss-of-function *Tet3* mutations (in 2 *ΔT2T3* mice).

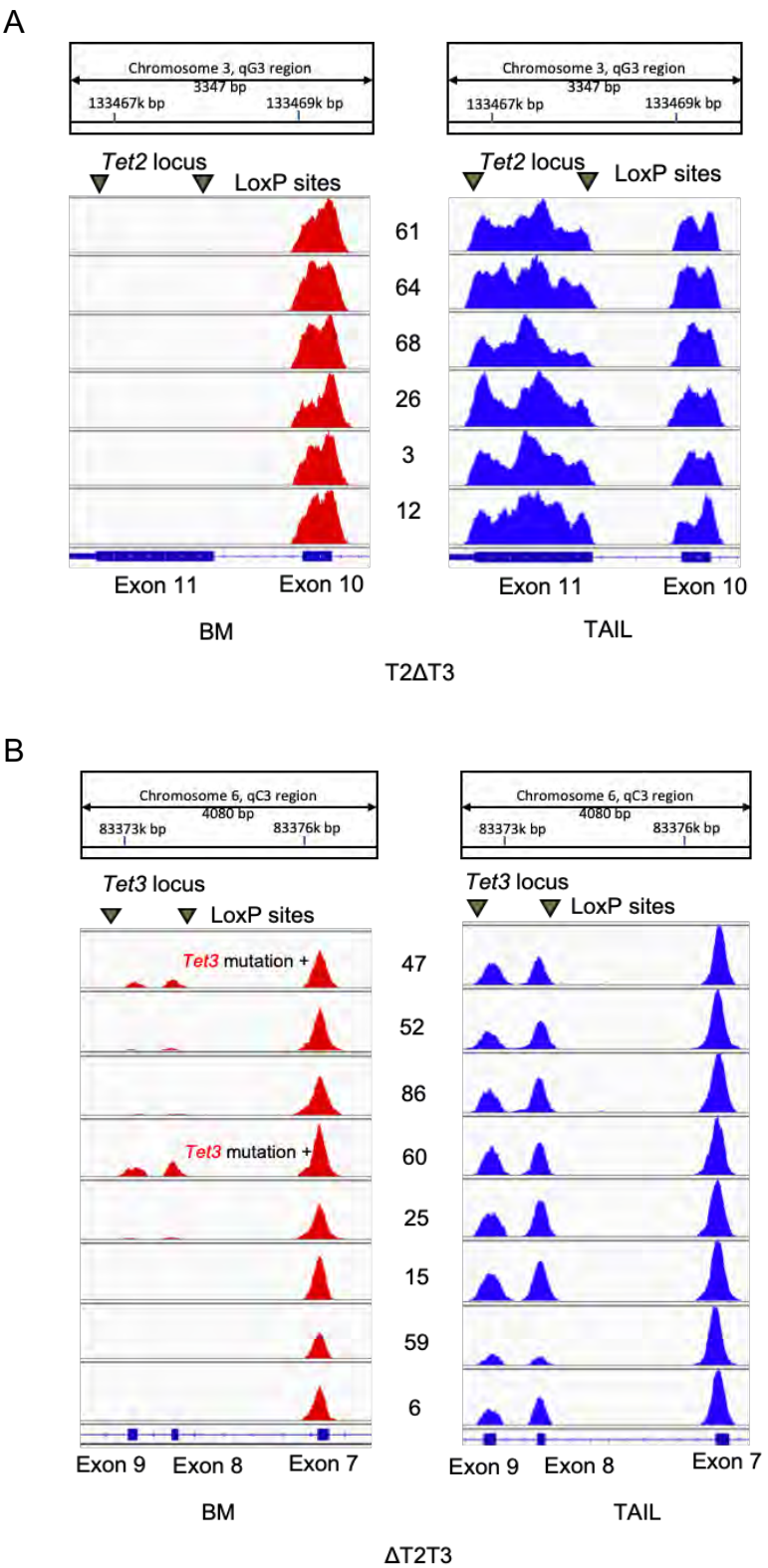

Figure 15: Graphical representation of exome sequencing of *T2ΔT3 and ΔT2T3* mice on Integrative Genomics Viewer (IGV).
IGV-inspected sequence reads of *Tet2* locus in *T2ΔT3* mice (A) and on *Tet3* locus in *ΔT2T3* mice (B) are shown for BM (red) and tail (blue) DNAs. Note that the absence of reads is shown for exon 11 of *Tet2* in leukemic BM of *T2ΔT3* mice (n = 6; A) and for exons 8 and 9 of *Tet3* in leukemic BM of *T2ΔT3* mice (n = 6; B). Reads were present in the BM of 2 *T2ΔT3* mice (#47 and #60). Probe tracks has been shown to indicate position on the chromosome; bp = base pairs, k=1000.

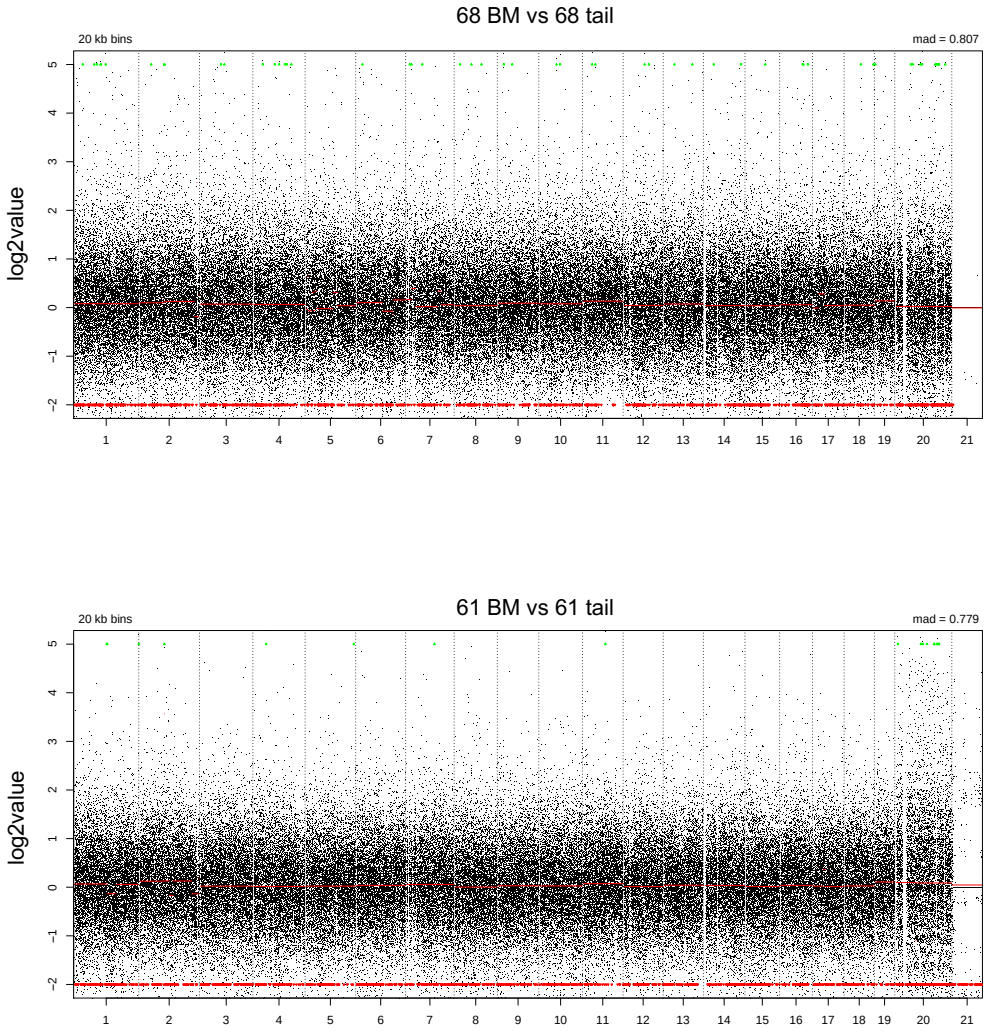

Figure 16: Copy number detection for exome sequencing data.
Representative figures of *ΔT2ΔT3, T2ΔT3 and ΔT2T3* mice showing copy number variation. Figures were generated after raw bam files from WES were applied to Copywrite R.

5.3 Loss of wild-type *Tet2* allele occurs before onset of full-blown AML development

To examine the deletion status of residual alleles during the time course of leukemia development, I performed multiplex PCR of myeloid, B, and T cells sorted from peripheral blood of *T2ΔT3* mice (n = 2) at 10 weeks. I continued to follow the PCR results at regular intervals of 8 weeks (Figure 17A). I also simultaneously performed flow cytometry for peripheral blood cells of these mice and observed a gradual increase in of CD11b/Gr1^{+} fraction (Figure 17B). I observed that at approximately 35 weeks of age, the wild-type *Tet2* band became invisible in the myeloid cells in these mice (Figure 17A). Mouse #10 showed WBC of 125 X 10^2/ul and hemoglobin of 10.7 g/dl, and mouse #12 showed WBC of 282 X 10^2/ul and hemoglobin of 11.9 g/dl (Figure 17C). These blood parameters did not fulfil our definition of leukemia (WBC >200 X 10^2/ul and hemoglobin <10 g/dl) but they indicated progression towards leukemia in these mice. It was concluded that loss of the remaining *Tet2* and *Tet3* allele is a relatively early event that eventually leads to full-blown leukemia.

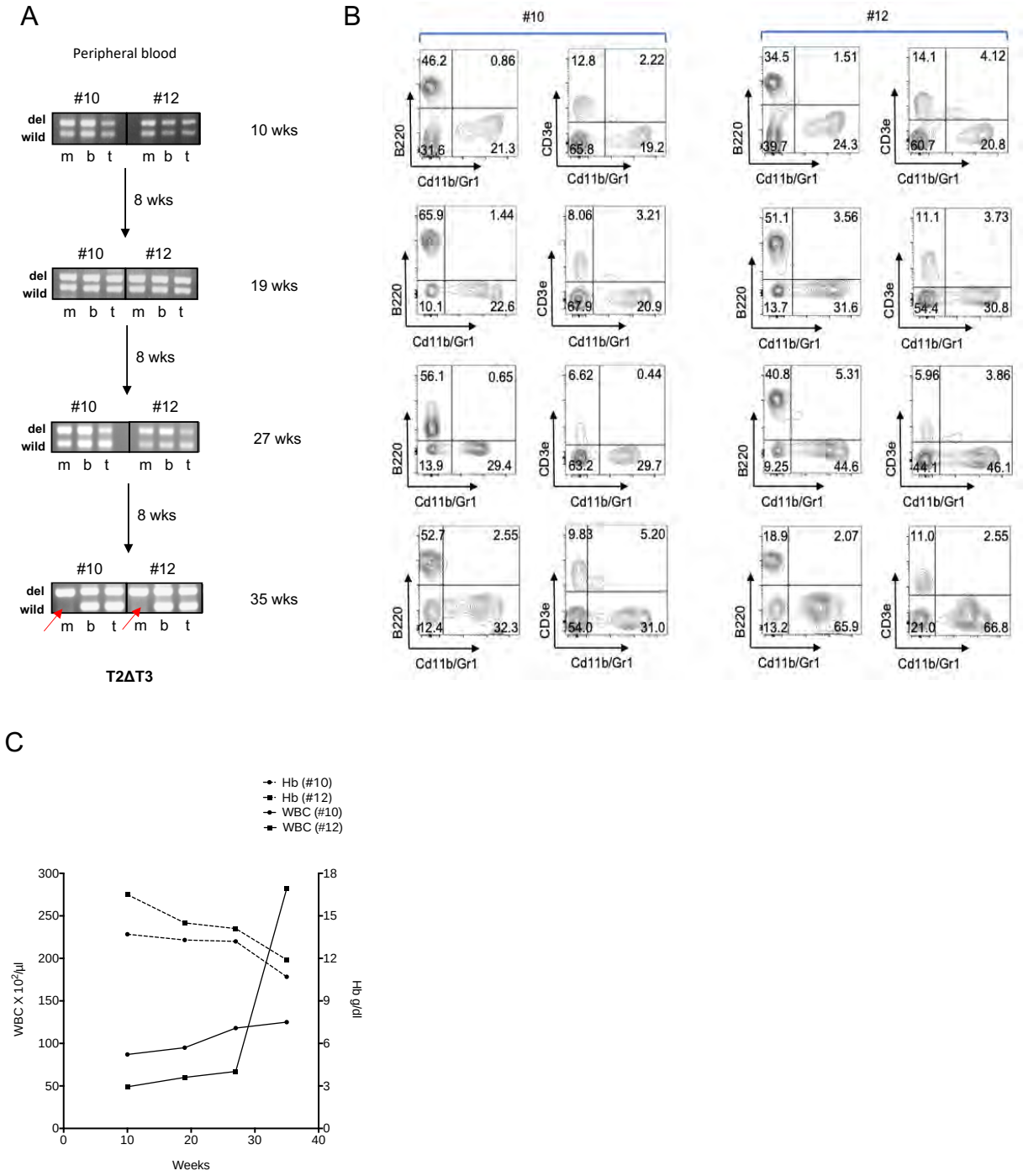

Figure 17: Follow ups to monitor loss of wild type *Tet2* band in T2ΔT3 mice.
(A) Multiplex PCR of myeloid (m), B (b) and T (t) cells sorted from peripheral blood of T2ΔT3 mice (n = 2; #10 and #12) performed at 10, 19, 27 and 35 weeks of age. Loss of *Tet2* wild-type allele is shown by red arrows. (B) Flow cytometry analysis of peripheral blood of T2ΔT3 mice (n = 2; #10 and #12) performed at 10, 19, 27 and 35 weeks of age. (C) Graphical representation of measurements of white blood cells and hemoglobin of T2ΔT3 mice (n = 2; #10 and #12) at 10, 19, 27 and 35 weeks of age.

6. Discussion

In this study, the phenotypic and genotypic characterization of AML that developed in mice with four-allele and three-allele disruption of *Tet2* and *Tet3* has been shown. The AML phenotype seen in both three-allele and four-allele disrupted mice were very similar in terms of cell surface antigen expression, penetrance of the diseases in the transplanted mice, and response to an HMA *in vitro*. However, the latencies were significantly longer in the three-allele deficient mice. This suggested the requirement of additional genetic events for leukemia development in these mice. I demonstrated that inactivation of the functional *Tet2* or *Tet3* allele was an extremely frequent event, as well as the only recurrent event, identified in AML cells supported by PCR and WES. As a result, AML genotype that developed in the three-allele disrupted mice closely resembled the genotype that developed in the four-allele disrupted mice. This further supported the resemblance of the AML phenotype in both the three- and the four-allele deficient mice.

As I did not observe any deletion of *Tet2* or *Tet3* in copy number analysis of the WES data, I think that uniparental disomy (UPD) may cause duplication of the region deleted by the loxP system, exon 11 of *Tet2,* and exons 8 and 9 of *Tet3*. It is known that *TET2* abnormalities in patients with hematologic malignancies are often biallelic, due to UPD, microdeletion plus SNV, and heterozygous SNVs.[31,36,39,60-63] Hence, the loss of the *Tet2* allele that frequently occurred in my mouse model is indeed not surprising. In AML patients, *TET2* mutations are often accompanied by other genetic mutations. However, concurrent identification of *TET2* and *TET3* mutations have been reported only in few cases.[64] The data derived from the TCGA dataset showed positive correlation between *TET2* and *TET3* mRNA expression levels. [53] This suggests that both *TET2* and *TET3* show low expression in a proportion of AML patients, which may contribute to drive AML development as we observed in mice. The observed correlation could be due to effect of *TET2* and *TET3* on each other. A study showed that *TET2* and *TET3*

had a combined requirement and overlapping roles in hematopoietic stem cell emergence and regulation [65] and they may cooperate to inhibit abnormal hematopoiesis. Further studies are necessary to understand how *TET2* and *TET3* closely work together in hematopoietic cells. The mechanism of development of AML in three-allele knockout mice in my study and the positive co-relation between mRNA expression of *TET2* and *TET3* from the TCGA dataset could suggest an interesting relationship between *TET3* expression and leukemia.

mRNA expression of *Tet3* has been shown to decline with age in mouse hematopoietic stem cells [43], as well as in human peripheral blood T cells. [44] Studies have shown that potential sources of *TET3* epigenetic downregulation could be DNA hypermethylation and loss of DNA hydroxymethylation, and reduction in activating histone marks that are associated with aging. [43,66] Such changes are likely to be conducive to transformative changes leading to myeloid leukemia. The effect of downregulation of *TET3* on the development of AML with increasing age needs to be further clarified and warrants further investigations.

As previously discussed, TET enzymes regulate the methylation status at the CpG sites of genomic DNA, mainly at the gene body.[67] In this regard, cytosine hypermethylation is seen in BM cells of patients with myeloid malignancies with *TET2* mutations.[68] Similarly, hypermethylation status has been reported in hematopoietic stem/progenitor cells (HSPC) of mice with four-allele deficiency of *Tet2* and *Tet3* genes.[45] Taken together, they indicate that the profound hypermethylation status induced by severe reduction of the enzymatic function of TET2 and TET3 may lead to development of full-blown AML. This observation is also strongly supported by the fact that no additional genetic mutations were identified in four-allele deficient AML cells by whole exome sequencing. Some nonrecurrent mutations in three-allele deficient mice, such as Set domain containing the 1b *(Setd1b)*, Catenin alpha 1 *(Ctnna1)*, Olfactory receptor *(Olfr152)*, Membrane organizing extension spike protein *(Msn)*, and

Multiple epidermal growth-factor like domains *(Megf11)*, have been identified in human AML cells and, thus, might have made contribution to an extent.[56,69-75]

Hypomethylating agents, decitabine and azacitidine (which is metabolized into decitabine intracellularly) inhibit DNA methyltransferases and decrease the methylation of cytosine residues. Though these agents have been approved for the treatment of myelodysplastic syndrome (MDS), their use in treatment of acute myeloid leukemia has been mostly limited to combination with other drugs.[76] Studies have reported varied overall response rate; 55% with decitabine in MDS patients with mutated *Tet2* [77] and 82% with azacitidine in MDS and AML with mutated *Tet2*.[78] However, response of decitabine in AML patients with *Tet2* mutation has not been reported yet.

The findings of my study emphasize that the remaining intact *Tet2* or *Tet3* allele may act as a sentinel to prevent HSC from AML progression. Some AML cells may indeed depend on the hypermethylation status induced by severely reduced TET enzymatic activity. These conditions could be explored as potential therapeutic targets by HMAs in future.

7. Conclusion

My study concludes that *Tet2*/*Tet3* three- and four-allele knockout mice developed AML with similar phenotypic and genotypic features but with variable latencies. Three-allele disrupted mice required additional secondary somatic mutations to progress to leukemia whereas four-allele disrupted mice spontaneously developed leukemia within a short period. This suggests that the residual *Tet2/Tet3* allele plays an important role as a gatekeeper that prevents the progression of leukemia.

8. Acknowledgement

I would like to express my sincere gratitude to my supervisor, Professor Shigeru Chiba and my academic advisor, Associate Professor Mamiko Sakata-Yanagimoto for their continuous guidance and support during my graduate studies. I am thankful to my previous colleagues Koichiro Maie and Masatomo Ishihara and all others who contributed towards the completion of this project. I would also like to extend my gratitude to my fellow colleagues and members of the hematology department for always lending me a hand and motivating me when necessary.

Most of all, I am very thankful to my dear husband, Mingma for his affection, relentless support and encouragement throughout the years. I am also grateful towards my family for their unconditional support.

9. Source

The contents previously published in *Blood Advances*. 2020;4(5):845-854. (doi:10.1182/bloodadvances.2019001324) are re-used in this dissertation following copyright information in *Blood Advances*. https://ashpublications.org/bloodadvances/pages/copyright

10. References

1. Döhner H, Weisdorf DJ, Bloomfield CD. Acute Myeloid Leukemia. Longo DL, ed. *N Engl J Med*. 2015;373(12):1136-1152. doi:10.1056/NEJMra1406184.

2. Liesveld JL, Lichtman MA. Acute myeloid leukemia. In: Kaushansky K, Lichtman MA, Prchal JT, et al., eds. *Williams Hematology*. 9th edition. New York: McGraw-Hill Education; 2016:1373-1436.

3. Yamamoto JF, Goodman MT. Patterns of leukemia incidence in the United States by subtype and demographic characteristics, 1997-2002. *Cancer Causes Control*. 2008;19(4):379-390. doi:10.1007/s10552-007-9097-2.

4. 足立 桂也, 石川 裕一, 清井 仁. 急性骨髄性白血病. In "Principles and Practice 血液・造血器・リンパ系" (編集：千葉 滋, 長谷川 雄一) 文光堂, 東京, 2015: 219-229.

5. Campos L, Guyotat D, Archimbaud E, et al. Surface marker expression in adult acute myeloid leukaemia: correlations with initial characteristics, morphology and response to therapy. *Br J Haematol*. 1989;72(2):161-166. doi:10.1111/j.1365-2141.1989.tb07677.x.

6. Döhner H, Estey EH, Amadori S, et al. Diagnosis and management of acute myeloid leukemia in adults: recommendations from an international expert panel, on behalf of the European LeukemiaNet. *Blood*. 2010;115(3):453-474. doi:10.1182/blood-2009-07-235358.

7. De Kouchkovsky I, Abdul-Hay M. 'Acute myeloid leukemia: a comprehensive review and 2016 update'. *Blood Cancer J*. 2016;6(7):e441-e441. doi:10.1038/bcj.2016.50.

8. Walker A, Marcucci G. Molecular prognostic factors in cytogenetically normal acute myeloid leukemia. *Expert Rev Hematol*. 2012;5(5):547-558. doi:10.1586/ehm.12.45.

9. DiNardo CD, Cortes JE. Mutations in AML: prognostic and therapeutic implications. *Hematology Am Soc Hematol Educ Program*. 2016;2016(1):348-355. doi:10.1182/asheducation-2016.1.348.

10. Shah A, Andersson TM-L, Rachet B, Björkholm M, Lambert PC. Survival and cure of acute myeloid leukaemia in England, 1971-2006: a population-based study. *Br J Haematol*. 2013;162(4):509-516. doi:10.1111/bjh.12425.

11. Meyers J, Yu Y, Kaye JA, Davis KL. Medicare fee-for-service enrollees with primary acute myeloid leukemia: an analysis of treatment patterns, survival, and healthcare resource utilization and costs. *Appl Health Econ Health Policy*. 2013;11(3):275-286. doi:10.1007/s40258-013-0032-2.

12. Ono R, Taki T, Taketani T, Taniwaki M, Kobayashi H, Hayashi Y. LCX, leukemia-associated protein with a CXXC domain, is fused to MLL in acute myeloid leukemia with trilineage dysplasia having t(10;11)(q22;q23). *Cancer Res*. 2002;62(14):4075-4080.

13. Lorsbach RB, Moore J, Mathew S, Raimondi SC, Mukatira ST, Downing JR. TET1, a member of a novel protein family, is fused to MLL in acute myeloid leukemia containing the t(10;11)(q22;q23). *Leukemia 2011 26:5*. 2003;17(3):637-641. doi:10.1038/sj.leu.2402834.

14. Zhang H, Zhang X, Clark E, Mulcahey M, Huang S, Shi YG. TET1 is a DNA-binding protein that modulates DNA methylation and gene transcription via hydroxylation of 5-methylcytosine. *Cell Res*. 2010;20(12):1390-1393. doi:10.1038/cr.2010.156.

15. Xu Y, Wu F, Tan L, et al. Genome-wide regulation of 5hmC, 5mC, and gene expression by Tet1 hydroxylase in mouse embryonic stem cells. *Mol Cell*. 2011;42(4):451-464. doi:10.1016/j.molcel.2011.04.005.

16. Xu Y, Xu C, Kato A, et al. Tet3 CXXC domain and dioxygenase activity cooperatively regulate key genes for Xenopus eye and neural development. *Cell*. 2012;151(6):1200-1213. doi:10.1016/j.cell.2012.11.014.

17. Baylin SB, Jones PA. A decade of exploring the cancer epigenome - biological and translational implications. *Nat Rev Cancer*. 2011;11(10):726-734. doi:10.1038/nrc3130.

18. Wu H, Zhang Y. Reversing DNA methylation: mechanisms, genomics, and biological functions. *Cell*. 2014;156(1-2):45-68. doi:10.1016/j.cell.2013.12.019.

19. Walsh CP, Xu GL. Cytosine methylation and DNA repair. *Curr Top Microbiol Immunol*. 2006;301(Chapter 11):283-315. doi:10.1007/3-540-31390-7_11.

20. Wu X, Zhang Y. TET-mediated active DNA demethylation: mechanism, function and beyond. *Nat Rev Genet*. 2017;18(9):517-534. doi:10.1038/nrg.2017.33.

21. Ito S, D'Alessio AC, Taranova OV, Hong K, Sowers LC, Zhang Y. Role of Tet proteins in 5mC to 5hmC conversion, ES-cell self-renewal and inner cell mass specification. *Nature*. 2010;466(7310):1129-1133. doi:10.1038/nature09303.

22. He Y-F, Li B-Z, Li Z, et al. Tet-mediated formation of 5-carboxylcytosine and its excision by TDG in mammalian DNA. *Science*. 2011;333(6047):1303-1307. doi:10.1126/science.1210944.

23. Tahiliani M, Koh KP, Shen Y, et al. Conversion of 5-methylcytosine to 5-hydroxymethylcytosine in mammalian DNA by MLL partner TET1. *Science*. 2009;324(5929):930-935. doi:10.1126/science.1170116.

24. Pastor WA, Aravind L, Rao A. TETonic shift: biological roles of TET proteins in DNA demethylation and transcription. *Nat Rev Mol Cell Biol*. 2013;14(6):341-356. doi:10.1038/nrm3589.

25. Dawlaty MM, Breiling A, Le T, et al. Combined deficiency of Tet1 and Tet2 causes epigenetic abnormalities but is compatible with postnatal development. *Dev Cell*. 2013;24(3):310-323. doi:10.1016/j.devcel.2012.12.015.

26. Kudo Y, Tateishi K, Yamamoto K, et al. Loss of 5-hydroxymethylcytosine is accompanied with malignant cellular transformation. *Cancer Sci*. 2012;103(4):670-676. doi:10.1111/j.1349-7006.2012.02213.x.

27. Lian CG, Xu Y, Ceol C, et al. Loss of 5-hydroxymethylcytosine is an epigenetic hallmark of melanoma. *Cell*. 2012;150(6):1135-1146. doi:10.1016/j.cell.2012.07.033.

28. Liu C, Liu L, Chen X, et al. Decrease of 5-hydroxymethylcytosine is associated with progression of hepatocellular carcinoma through downregulation of TET1. Guan X-Y, ed. *PLoS ONE*. 2013;8(5):e62828. doi:10.1371/journal.pone.0062828.

29. Yang H, Liu Y, Bai F, et al. Tumor development is associated with decrease of TET gene expression and 5-methylcytosine hydroxylation. *Oncogene*. 2013;32(5):663-669. doi:10.1038/onc.2012.67.

30. Huang H, Jiang X, Li Z, et al. TET1 plays an essential oncogenic role in MLL-rearranged leukemia. *Proc Natl Acad Sci USA*. 2013;110(29):11994-11999. doi:10.1073/pnas.1310656110.

31. Delhommeau F, Dupont S, Valle Della V, et al. Mutation in TET2 in myeloid cancers. *N Engl J Med*. 2009;360(22):2289-2301. doi:10.1056/NEJMoa0810069.

32. Metzeler KH, Maharry K, Radmacher MD, et al. TET2 mutations improve the new European LeukemiaNet risk classification of acute myeloid leukemia: a Cancer and Leukemia Group B study. *J Clin Oncol*. 2011;29(10):1373-1381. doi:10.1200/JCO.2010.32.7742.

33. Cancer Genome Atlas Research Network, Ley TJ, Miller C, et al. Genomic and epigenomic landscapes of adult de novo acute myeloid leukemia. *N Engl J Med*. 2013;368(22):2059-2074. doi:10.1056/NEJMoa1301689.

34. Weissmann S, Alpermann T, Grossmann V, et al. Landscape of TET2 mutations in acute myeloid leukemia. *Leukemia 2011 26:5*. 2012;26(5):934-942. doi:10.1038/leu.2011.326.

35. Figueroa ME, Abdel-Wahab O, Lu C, et al. Leukemic IDH1 and IDH2 mutations result in a hypermethylation phenotype, disrupt TET2 function, and impair hematopoietic differentiation. *Cancer Cell*. 2010;18(6):553-567. doi:10.1016/j.ccr.2010.11.015.

36. Langemeijer SMC, Kuiper RP, Berends M, et al. Acquired mutations in TET2 are common in myelodysplastic syndromes. *Nat Genet*. 2009;41(7):838-842. doi:10.1038/ng.391.

37. Bejar R, Stevenson K, Abdel-Wahab O, et al. Clinical effect of point mutations in myelodysplastic syndromes. *N Engl J Med*. 2011;364(26):2496-2506. doi:10.1056/NEJMoa1013343.

38. Haferlach T, Nagata Y, Grossmann V, et al. Landscape of genetic lesions in 944 patients with myelodysplastic syndromes. *Leukemia 2011 26:5*. 2014;28(2):241-247. doi:10.1038/leu.2013.336.

39. Tefferi A, Pardanani A, Lim K-H, et al. TET2 mutations and their clinical correlates in polycythemia vera, essential thrombocythemia and myelofibrosis. *Leukemia 2011 26:5*. 2009;23(5):905-911. doi:10.1038/leu.2009.47.

40. Jaiswal S, Fontanillas P, Flannick J, et al. Age-related clonal hematopoiesis associated with adverse outcomes. *N Engl J Med*. 2014;371(26):2488-2498. doi:10.1056/NEJMoa1408617.

41. Jan M, Snyder TM, Corces-Zimmerman MR, et al. Clonal evolution of preleukemic hematopoietic stem cells precedes human acute myeloid leukemia. *Sci Transl Med*. 2012;4(149):149ra118-149ra118. doi:10.1126/scitranslmed.3004315.

42. Xie M, Lu C, Wang J, et al. Age-related mutations associated with clonal hematopoietic expansion and malignancies. *Nat Med*. 2014;20(12):1472-1478. doi:10.1038/nm.3733.

43. Sun D, Luo M, Jeong M, et al. Epigenomic profiling of young and aged HSCs reveals concerted changes during aging that reinforce self-renewal. *Cell Stem Cell*. 2014;14(5):673-688. doi:10.1016/j.stem.2014.03.002.

44. Truong TP, Sakata-Yanagimoto M, Yamada M, et al. Age-Dependent Decrease of DNA Hydroxymethylation in Human T Cells. *J Clin Exp Hematop*. 2015;55(1):1-6. doi:10.3960/jslrt.55.1.

45. An J, González-Avalos E, Chawla A, et al. Acute loss of TET function results in aggressive myeloid cancer in mice. *Nat Commun*. 2015;6(1):10071. doi:10.1038/ncomms10071.

46. Quivoron C, Couronné L, Valle Della V, et al. TET2 inactivation results in pleiotropic hematopoietic abnormalities in mouse and is a recurrent event during human lymphomagenesis. *Cancer Cell*. 2011;20(1):25-38. doi:10.1016/j.ccr.2011.06.003.

47. Ko M, An J, Pastor WA, Koralov SB, Rajewsky K, Rao A. TET proteins and 5-methylcytosine oxidation in hematological cancers. *Immunol Rev*. 2015;263(1):6-21. doi:10.1111/imr.12239.

48. Moran-Crusio K, Reavie L, Shih A, et al. Tet2 loss leads to increased hematopoietic stem cell self-renewal and myeloid transformation. *Cancer Cell*. 2011;20(1):11-24. doi:10.1016/j.ccr.2011.06.001.

49. Li Z, Cai X, Cai C-L, et al. Deletion of Tet2 in mice leads to dysregulated hematopoietic stem cells and subsequent development of myeloid malignancies. *Blood*. 2011;118(17):4509-4518. doi:10.1182/blood-2010-12-325241.

50. Muto H, Sakata-Yanagimoto M, Nagae G, et al. Reduced TET2 function leads to T-cell lymphoma with follicular helper T-cell-like features in mice. *Blood Cancer J*. 2014;4(12):e264-e264. doi:10.1038/bcj.2014.83.

51. Mouly E, Ghamlouch H, Valle Della V, et al. B-cell tumor development in Tet2-deficient mice. *Blood Adv*. 2018;2(6):703-714. doi:10.1182/bloodadvances.2017014118.

52. Dominguez PM, Ghamlouch H, Rosikiewicz W, et al. TET2 Deficiency Causes Germinal Center Hyperplasia, Impairs Plasma Cell Differentiation, and Promotes B-cell Lymphomagenesis. *Cancer Discov*. 2018;8(12):1632-1653. doi:10.1158/2159-8290.CD-18-0657.

53. 真家 紘一郎. *Tet2*と*Tet3*の二重欠損マウスは脱メチル化薬感受性の急性骨髄性白血病を発症する. 筑波大学博士（医学）学位論文, 2018.

54. 石原 昌朋. *Tet2*及び*Tet3*遺伝子は協調して造血細胞の腫瘍発症抑制に働くか. 筑波大学修士（医科学）学位論文, 2018.

55. Kühn R, Schwenk F, Aguet M, Rajewsky K. Inducible gene targeting in mice. *Science*. 1995;269(5229):1427-1429. doi:10.1126/science.7660125.

56. Kotani S, Yoda A, Kon A, et al. Molecular pathogenesis of disease progression in MLL-rearranged AML. *Leukemia 2011 26:5*. 2019;33(3):612-624. doi:10.1038/s41375-018-0253-3.

57. Li H, Durbin R. Fast and accurate short read alignment with Burrows-Wheeler transform. *Bioinformatics*. 2009;25(14):1754-1760. doi:10.1093/bioinformatics/btp324.

58. Kuilman T, Velds A, Kemper K, et al. CopywriteR: DNA copy number detection from off-target sequence data. *Genome Biol*. 2015;16(1):49–15. doi:10.1186/s13059-015-0617-1.

59. Kent WJ. BLAT--the BLAST-like alignment tool. *Genome Res*. 2002;12(4):656-664. doi:10.1101/gr.229202.

60. Tefferi A, Lim K-H, Abdel-Wahab O, et al. Detection of mutant TET2 in myeloid malignancies other than myeloproliferative neoplasms: CMML, MDS, MDS/MPN and AML. *Leukemia 2011 26:5*. 2009;23(7):1343-1345. doi:10.1038/leu.2009.59.

61. Jankowska AM, Szpurka H, Tiu RV, et al. Loss of heterozygosity 4q24 and TET2 mutations associated with myelodysplastic/myeloproliferative neoplasms. *Blood*. 2009;113(25):6403-6410. doi:10.1182/blood-2009-02-205690.

62. Abdel-Wahab O, Mullally A, Hedvat C, et al. Genetic characterization of TET1, TET2, and TET3 alterations in myeloid malignancies. *Blood*. 2009;114(1):144-147. doi:10.1182/blood-2009-03-210039.

63. Kosmider O, Gelsi-Boyer V, Ciudad M, et al. TET2 gene mutation is a frequent and adverse event in chronic myelomonocytic leukemia. *Haematologica*. 2009;94(12):1676-1681. doi:10.3324/haematol.2009.011205.

64. Merlevede J, Droin N, Qin T, et al. Mutation allele burden remains unchanged in chronic myelomonocytic leukaemia responding to hypomethylating agents. *Nat Commun*. 2016;7(1):10767. doi:10.1038/ncomms10767.

65. Li C, Lan Y, Schwartz-Orbach L, et al. Overlapping Requirements for Tet2 and Tet3 in Normal Development and Hematopoietic Stem Cell Emergence. *Cell Rep*. 2015;12(7):1133-1143. doi:10.1016/j.celrep.2015.07.025.

66. Carella A, Tejedor JR, García MG, et al. Epigenetic downregulation of TET3 reduces genome-wide 5hmC levels and promotes glioblastoma tumorigenesis. *Int J Cancer*. 2020;146(2):373-387. doi:10.1002/ijc.32520.

67. Rasmussen KD, Jia G, Johansen JV, et al. Loss of TET2 in hematopoietic cells leads to DNA hypermethylation of active enhancers and induction of leukemogenesis. *Genes Dev*. 2015;29(9):910-922. doi:10.1101/gad.260174.115.

68. Pérez C, Martínez-Calle N, Martín-Subero JI, et al. TET2 mutations are associated with specific 5-methylcytosine and 5-hydroxymethylcytosine profiles in patients with chronic myelomonocytic leukemia. Ballestar E, ed. *PLoS ONE*. 2012;7(2):e31605. doi:10.1371/journal.pone.0031605.

69. Yang W, Ernst P. SET/MLL family proteins in hematopoiesis and leukemia. *Int J Hematol*. 2017;105(1):7-16. doi:10.1007/s12185-016-2118-8.

70. Tiziana Storlazzi C, Pieri L, Paoli C, et al. Complex karyotype in a polycythemia vera patient with a novel SETD1B/GTF2H3 fusion gene. *Am J Hematol*. 2014;89(4):438-442. doi:10.1002/ajh.23659.

71. Huang Y, Rao A. Connections between TET proteins and aberrant DNA modification in cancer. *Trends Genet*. 2014;30(10):464-474. doi:10.1016/j.tig.2014.07.005.

72. Couronné L, Bastard C, Bernard OA. TET2 and DNMT3A mutations in human T-cell lymphoma. *N Engl J Med*. 2012;366(1):95-96. doi:10.1056/NEJMc1111708.

73. Manteniotis S, Wojcik S, Brauhoff P, et al. Functional characterization of the ectopically expressed olfactory receptor 2AT4 in human myelogenous leukemia. *Cell Death Discov*. 2016;2(1):15070. doi:10.1038/cddiscovery.2015.70.

74. Manteniotis S, Wojcik S, Göthert JR, et al. Deorphanization and characterization of the ectopically expressed olfactory receptor OR51B5 in myelogenous leukemia cells. *Cell Death Discov*. 2016;2(1):16010. doi:10.1038/cddiscovery.2016.10.

75. Vosberg S, Hartmann L, Metzeler KH, et al. Relapse of acute myeloid leukemia after allogeneic stem cell transplantation is associated with gain of WT1 alterations and high mutation load. *Haematologica*. 2018;103(12):e581-e584. doi:10.3324/haematol.2018.193102.

76. DiNardo CD, Pratz K, Pullarkat V, et al. Venetoclax combined with decitabine or azacitidine in treatment-naive, elderly patients with acute myeloid leukemia. *Blood*. 2019;133(1):7-17. doi:10.1182/blood-2018-08-868752.

77. Bejar R, Lord A, Stevenson K, et al. TET2 mutations predict response to hypomethylating agents in myelodysplastic syndrome patients. *Blood*. 2014;124(17):2705-2712. doi:10.1182/blood-2014-06-582809.

78. Itzykson R, Kosmider O, Cluzeau T, et al. Impact of TET2 mutations on response rate to azacitidine in myelodysplastic syndromes and low blast count acute myeloid leukemias. *Leukemia 2011 26:5*. 2011;25(7):1147-1152. doi:10.1038/leu.2011.71.